Atmos. Chem. Phys. Discuss., https://doi.org/10.5194/acp-2018-148
Manuscript under review for journal Atmos. Chem. Phys.
Discussion started: 13 February 2018

Atmospheric Chemistry and Physics Discussions

Changes in the aerosol direct radiative forcing from 2001 to 2015: observational constraints and regional mechanisms

Fabien Paulot[1,2], David Paynter[1], Paul Ginoux[1], Vaishali Naik[1], and Larry W. Horowitz[1]

[1]Geophysical Fluid Dynamics Laboratory, National Oceanic and Atmospheric Administration, Princeton, New Jersey, USA

[2]Program in Atmospheric and Oceanic Sciences, Princeton University, New Jersey, USA

Correspondence to: Fabien.Paulot@noaa.gov

Abstract. We present observation and model-based estimates of the changes in the direct shortwave effect of aerosols under clear-sky (SDRECS) from 2001 to 2015. Observation-based estimates are obtained from changes in the outgoing shortwave clear-sky radiation (Rsutcs) measured by the Clouds and the Earth's Radiant Energy System (CERES), accounting for the effect of variability in surface albedo, water vapor, and ozone. We find increases in SDRECS (i.e., less radiation scattered to space by aerosols) over Western Europe (0.7 – 1 $\mathrm{W\,m^{-2}\,dec^{-1}}$) and the Eastern US (0.9 – 1.8 $\mathrm{W\,m^{-2}\,dec^{-1}}$), decreases over India (-0.5 – -1.9 $\mathrm{W\,m^{-2}\,dec^{-1}}$) and no significant change over Eastern China. Comparisons with the GFDL chemistry climate model AM3, driven by CMIP6 historical emissions, show that changes in SDRECS over Western Europe and the Eastern US are well captured, which largely reflects the mature understanding of the sulfate budget in these regions. In contrast, the model overestimates the trends in SDRECS over India and Eastern China. Over China, this bias can be partly attributed to the decline of SO_2 emissions after 2007, which is not captured by the CMIP6 emissions. In both India and Eastern China, we find much larger contributions of nitrate and black carbon to changes in SDRECS than in the US and Europe, which highlights the need to better constrain their precursors and chemistry. Globally, our model shows that changes in the all-sky aerosol direct forcing between 2001 and 2015 (+0.03 $\mathrm{W\,m^{-2}}$) are dominated by black carbon (+0.12 $\mathrm{W\,m^{-2}}$) with significant offsets from nitrate (-0.03 $\mathrm{W\,m^{-2}}$) and sulfate (-0.03 $\mathrm{W\,m^{-2}}$). Changes in the sulfate (+7%) and nitrate (+60%) all-sky direct forcing between 2001 and 2015 are only weakly related to changes in the emissions of their precursors (-12.5% and 19% for SO_2 and NH_3, respectively), due mostly to chemical non linearities.

Atmos. Chem. Phys. Discuss., https://doi.org/10.5194/acp-2018-148
Manuscript under review for journal Atmos. Chem. Phys.
Discussion started: 13 February 2018

Atmospheric Chemistry and Physics Discussions

1 Introduction

Aerosols affect climate (Boucher et al., 2013) both directly, via scattering and absorption of incoming and outgoing radiation (Charlson et al., 1992), and indirectly, by modulating the abundance of cloud condensation nuclei, the droplet size distribution, and the lifetime of clouds (Twomey, 1974; Rosenfeld et al., 2014). Storelvmo et al. (2016) estimated that the increase in the burden of atmospheric aerosols associated with anthropogenic activities has masked approximately one third of the continental warming from greenhouse gases from 1964 to 2010, with important implications for global and regional climate (Wild, 2009; Bollasina et al., 2011). In this work, we focus on the aerosol direct forcing.

Multi-model comparisons suggest that the direct aerosol forcing, i.e., the direct perturbation of the Earth's radiative budget by anthropogenic aerosols, was -0.27 $\mathrm{W\,m^{-2}}$ in 2000 relative to 1850 (Myhre et al., 2013). However the large spread among models (-0.016 – -0.58 $\mathrm{W\,m^{-2}}$), complicates the assessment of the climate impact of anthropogenic aerosols. Previous studies have leveraged global spaceborne observations of the Earth Radiative budget (EOS) (Wielicki et al., 1996, 1998) and aerosol abundance (Kahn et al., 2005; Levy et al., 2013b) to estimate the overall aerosol radiative effect (Christopher and Zhang, 2004; Patadia et al., 2008; Loeb and Manalo-Smith, 2005; Kahn, 2012). However, estimates of the aerosol forcing, the anthropogenic component of the aerosol effect, remain primarily model based, as global observations cannot directly distinguish anthropogenic and natural aerosols (Su et al., 2013; Bellouin et al., 2005, 2008).

Here, we focus on the relationship between anthropogenic emissions and direct aerosol forcing (Stevens and Schwartz, 2012) and we examine whether significant changes in anthropogenic emissions over the key source regions of Europe, North America, China, and India over the 2001–2015 periods have affected the regional aerosol shortwave direct effect under clear-sky (SDRECS), where changes in SDRECS are constrained by the observed variability in outgoing shortwave radiation, surface albedo, ozone, and water vapor. A further motivation is to assess whether a state-of-the-art chemistry climate model (Geophysical Fluid Dynamic Laboratory (GFDL) AM3) driven by the latest emission from the Coupled Model Intercomparison Project (phase 6) can reproduce these observations. In particular, we show that the chemical speciation of SDRECS derived using AM3 can help understand differences in the regional response of SDRECS to emission changes. Finally we compare the sensitivity of the direct aerosol radiative forcing to emission changes from 2001 to 2015 with the longer-term change between 1850 and 2001.

Atmos. Chem. Phys. Discuss., https://doi.org/10.5194/acp-2018-148
Manuscript under review for journal Atmos. Chem. Phys.
Discussion started: 13 February 2018

Atmospheric Chemistry and Physics Discussions

2 Methods

2.1 GFDL-AM3 model

We use the GFDL-AM3 model (Donner et al., 2011; Naik et al., 2013), the atmospheric chemistry climate component of the GFDL-CM3 model (Donner et al., 2011; Griffies et al., 2011; John et al., 2012). The model is run from 2000 to 2015, using the first year as spin-up. The model horizontal resolution is $\simeq$ 200 km with 48 vertical levels. To facilitate comparisons with synoptic observations, the model horizontal winds are nudged to 6-hourly horizontal winds from the National Centers for Environmental Predication reanalysis (Kalnay et al., 1996). Monthly sea surface temperature and sea ice concentration are prescribed following Taylor et al. (2000) and Rayner et al. (2003), respectively. The configuration of AM3 used in this study includes recent improvements to the representation of the wet scavenging of chemical tracers by snow and convective precipitation (Liu et al., 2011; Paulot et al., 2016) and to the treatment of sulfate and nitrate chemistry (Paulot et al., 2016). We refer the reader to Paulot et al. (2016, 2017a) for detailed evaluation of this configuration of AM3.

The radiative transfer scheme takes into account the aerosol optical properties of sulfate, sea salt, dust, black carbon, organic carbon (Donner et al., 2011) and nitrate (Paulot et al., 2017b). Aerosols are assumed to be externally mixed, except for hydrophilic black carbon and sulfate (Donner et al., 2011). Hygroscopic growth is capped at 95% for all aerosols.

We use the anthropogenic emissions developed by the Community Emission Data System (CEDS v2017-05-18) for the Coupled Model Intercomparison Project Phase 6 (CMIP 6 (Hoesly et al., 2018)). As anthropogenic emissions are available until 2014 from CEDS, we repeat CEDS 2014 anthropogenic emissions for 2015. Monthly biomass burning emissions are based on the Global Fire Emissions Database (van Marle et al., 2017) and distributed vertically following Dentener et al. (2006). Natural emissions are based on Naik et al. (2013), except for isoprene emissions, which are calculated interactively using the Model of Emissions of Gases and Aerosols from Nature (Guenther et al., 2006).

Fig. 1 shows regional and global trends in the anthropogenic emissions of SO_2, NH_3, BC, and NO from 2001 to 2015. In the US and Europe, there have been significant declines in SO_2 (-71% and -66%, respectively) and NO (-48% and -39%) emissions, while NH_3 and BC emissions have changed little (<15%). In contrast, Chinese emissions of SO_2, NO, and BC have increased by 56%, 69%, and 93%, respectively, while Indian emissions of SO_2, NO, and BC have increased by 89%, 39%, and 89%. In India, ammonia emissions are larger relative to precursors of acidic aerosols (NO and SO_2) than in the US and Europe. Globally, emissions of NH_3, BC, and NO increase by 18%, 36%, and 16% over the 2001-2015 period, respectively. SO_2 emissions are nearly stable, peaking in 2006.

Atmos. Chem. Phys. Discuss., https://doi.org/10.5194/acp-2018-148
Manuscript under review for journal Atmos. Chem. Phys.
Discussion started: 13 February 2018

Atmospheric Chemistry and Physics Discussions

2.2 Aerosol optical depth

We use monthly aerosol optical depth from the Multi-angle Imaging SpectroRadiometer (MISR) at 555nm (Kahn et al., 2005, 2010) and the Moderate Resolution Imaging Spectroradiometer (MODIS) instruments on board the AQUA and TERRA satellites at 550 nm (collection 6, level3, merged deep blue/dark target) (Levy et al., 2013a; Sayer et al., 2014). Because of our focus on interannual variability, we neglect diurnal variations in AOD when comparing monthly model AOD with the different satellite products.

2.3 Aerosol shortwave direct effect

The instantaneous aerosol direct radiative effect (DRE) is defined as the difference between the outgoing radiation in the absence (Rutaf) and in the presence (Rut) of aerosols at the top of the atmosphere (TOA).

To better isolate the effect of aerosol variability on radiative fluxes, we focus on the aerosol direct shortwave radiative effect under clear-sky conditions (SDRECS).

$$SDRECS = Rsutcsaf - Rsutcs \tag{1}$$

where Rsutcs and Rsutcsaf are the outgoing clear-sky shortwave radiation with and without aerosols, respectively. Note that an increase of SDRECS indicates a decrease of the radiation scattered to space by aerosols.

2.3.1 Model-derived SDRECS

In AM3, we estimate SDRECS by calling the radiative transfer scheme twice, with and without aerosols (Paulot et al., 2017b) in the absence of clouds. Similarly, the instantaneous radiative effects of individual aerosol components ($\mathrm{SDRECS}_{\mathrm{AM3}}(x)$) is estimated as the difference in Rsut with and without aerosol x, where x can be sulfate (SUL), nitrate (NIT), black carbon (BC), organic carbon, dust, sea salt, and stratospheric volcanic aerosols. In the following, we will focus primarily on changes in sulfate and nitrate, which dominate changes in aerosol scattering, and black carbon, which dominates changes in aerosol absorption in AM3.

2.3.2 Observation-based SDRECS

In this section, we present three observation-based estimates of the variability in SDRECS from 2001 to 2015. All estimates described in this section are based upon the observed broadband radiance from the Clouds and the Earth's Radiant Energy System (CERES) (Wielicki et al., 1996, 1998).

A first estimate of SDRECS can be obtained using using equation (1) and the calculated Rsutcs and Rsutcsaf from the CERES Synoptic Radiative Fluxes product (SYN, edition 4a). In CERES-SYN, both terms are calculated using a radiative transfer code constrained by the outgoing CERES

Atmos. Chem. Phys. Discuss., https://doi.org/10.5194/acp-2018-148
Manuscript under review for journal Atmos. Chem. Phys.
Discussion started: 13 February 2018

TOA shortwave radiative flux (Rsut), and estimates for aerosol optical properties, precipitable water (WVP), and ozone (qo3). WVP and qo3 are from the Goddard Modeling and Assimilation Office (GMAO) GEOS5 reanalysis. Aerosol optical properties are from the Model for Atmospheric Transport and Chemistry (MATCH) model (Collins et al., 2001) constrained by MODIS AOD (collection 5). The CERES-SYN estimate of SDRECS will be referred to as $\mathrm{SDRECS_{CS}}$ hereafter.

A separate estimate of the variability in SDRECS can be derived using observations of Rsutcs from the CERES Energy Balanced and Filled product (EBAF, edition 4, (Loeb et al., 2009)). This product achieves global coverage for Rsutcs by combining CERES broadband cloud-free fluxes with estimates of Rsutcs from MODIS (at 1km resolution) for regions that are not completely cloud-free at the CERES footprint scale (20 km) (CERES, 2017). We will use the subscript CE to refer to the CERES EBAF product hereafter.

Rsutcsaf will contain changes dues to non-aerosol components (Stevens and Schwartz, 2012; Xing et al., 2015). Therefore, if we are to use equation (1) to estimate the variability in SDRECS, we need to estimate the variability in Rsutcsaf. Here we assume that that it is linearly related to the variability in surface albedo (salb), water vapor, and ozone column:

$$\Delta_{m,y}\left(Rsutcsaf\right) = \Delta_{m,y}((\alpha \cdot salb + \beta \cdot WVP + \gamma \cdot qo3) \cdot Rsdt) \tag{2}$$

where $\alpha = \frac{\partial palb}{\partial salb}$, $\beta = \frac{\partial palb}{\partial WVP}$ and $\gamma = \frac{\partial palb}{\partial qo3}$. Rsdt and palb are the incoming shortwave flux at the top of the atmosphere and the planetary albedo, respectively. $\Delta_{m,y}(x)$ is the anomaly in x for month m and year y ($\Delta_{m,y}(x) = x_{m,y} - \frac{1}{15}\sum_{y=2001}^{2015} x_{m,y}$). Monthly gridded estimates of α, β, and γ are obtained from AM3.

We evaluate our methodology by showing that the variability in Rsutcsaf calculated in SYN ($\mathrm{Rsutcsaf_{CS}}$) can be estimated using equation (2). Figure 2 shows the root mean square (RMS) of the annual anomaly in $\mathrm{Rsutcsaf_{CS}}$ (panel A) and how it is reduced by applying in succession the correction terms on the right hand side of equation 2. Correcting for changes in the salb reduces the RMS over most land regions (Figure 2B). However, the RMS remains large over the Sahara, Australia, the Amazon, and North America. It is further reduced once changes in water vapor and to a lesser extend ozone are accounted for (Figure 2C and D). This gives us confidence in our ability to reproduce the variability in SDRECS calculated by the CERES SYN radiative transfer code when using the same albedo, water vapor, and ozone as used in the CERES SYN calculations. However, CERES EBAF flux is measured and not calculated. Therefore the accuracy of our estimates for $\mathrm{\Delta_{m,y}Rstucsaf}$ depends upon the accuracy of the estimates for surface albedo, water vapor, and ozone.

Figure 2 shows that $\mathrm{\Delta_{m,y}Rstucsaf}$ is most sensitive to $\mathrm{\Delta_{m,y}(salb)}$, so we use two independent estimates of surface albedo derived from CERES EBAF ($\mathrm{salb_{CE}}$) and MODIS ($\mathrm{salb_{M}}$). The associated estimates of SDRECS will be denoted as $\mathrm{SDRECS_{CE}}$ and $\mathrm{SDRECS_{M}}$, respectively, hereafter. We use GEOS5 for WVP and qo3, similar to CERES SYN.

Atmos. Chem. Phys. Discuss., https://doi.org/10.5194/acp-2018-148
Manuscript under review for journal Atmos. Chem. Phys.
Discussion started: 13 February 2018

Atmospheric Chemistry and Physics Discussions

The MODIS albedo (MCD43C3) ($\mathrm{salb_M}$) (Schaaf et al., 2002) is derived using the estimated reflectivity of the surface in the absence of aerosols in 7 MODIS spectral bands (Vermote et al., 1997, 2002; Vermote and Saleous, 2006; Vermote and Kotchenova, 2008). We use the estimates of the direct (black sky) and diffuse (white sky) albedo in both the near infrared and visible. Similar to Oleson et al. (2003), we consider the derived albedo regardless of the quality flag. The CERES surface broadband albedo ($salb_{CE}$) is estimated by finding the surface albedo that is most consistent with Rsutcs given constraints on aerosols from MATCH (Rutan et al., 2009, 2015), water vapor and ozone from GEOS5, and the spectral shape of the albedo. Both albedo estimates have been validated extensively and generally show good agreement with observations (Cescatti et al., 2012; Wang et al., 2014b; Rutan et al., 2009, 2015).

2.4 Trend characterization

Trend significance is determined using the non-parametric Mann-Kendall τ at p=0.05 (Kendall, 1938). This test is well-suited to the analysis of environmental datasets as it does not require residuals to be normally distributed. When a significant trend is detected, we calculate the linear trend using the Theil-Sen method (Theil, 1950; Sen, 1968).

3 Results

3.1 Spatial distribution of changes in SDRECS

Fig. 3 shows the decadal rate of change in outgoing shortwave radiation ($\mathrm{W\,m^{-2}\,dec^{-1}}$) measured by CERES EBAF (top panel, plotted as -Rsutcs for consistency with the definition of SDRECS) over the 2001–2015 period. Robust trends (dots) are detected in the outflow of the Eastern US (decrease in the shortwave radiation scattered to space) and in the outflow of India (increase in the shortwave radiation scattered to space), consistent with changes in aerosol precursors in these regions (Fig. 1). However, trends in Rsutcs are less robust and more heterogeneous over the source regions themselves, which suggests that other factors contribute to Rsutcs variability (Stevens and Schwartz, 2012; Xing et al., 2015).

Fig. 3 also shows the decadal rate of change in the different observation-based estimates of SDRECS described in section 2.3.2 ($\mathrm{SDRECS_M}$, $\mathrm{SDRECS_{CE}}$, $\mathrm{SDRECS_{CS}}$). All show better spatial consistency between land and ocean near large sources of anthropogenic pollution than Rsutcs. In particular, they show a significant increase in SDRECS over North America and Europe, and a significant decrease over India. In contrast, estimates of SDRECS show little variability over Australia, Kazakhstan, and South America, which suggests that the variability in Rsutcs is not primarily associated with aerosols in these regions. AM3 also shows increases in SDRECS over the US and Europe and decreases over India. However, it simulates a large decrease in SDRECS over China and in the Western Pacific, which is inconsistent with observational estimates.

Atmos. Chem. Phys. Discuss., https://doi.org/10.5194/acp-2018-148
Manuscript under review for journal Atmos. Chem. Phys.
Discussion started: 13 February 2018

Atmospheric Chemistry and Physics Discussions

3.2 Regional changes

Fig. 4 shows the annual anomalies in -Rsutcs (blue dashed line) and SDRECS (solid lines) over the Eastern US, Europe, India, and Eastern China. Rsutcs exhibits considerable interannual variability over the Eastern US and Europe, with no significant trend (Table S1). In contrast, all observational estimates of SDRECS exhibit a significant increase, i.e., a reduction of the radiation scattered to space by aerosols, ranging from 0.9 to 1.8 $\mathrm{W\,m^{-2}\,dec^{-1}}$ in the Eastern US and from 0.7 to 1.4 $\mathrm{W\,m^{-2}\,dec^{-1}}$ in Western Europe. The magnitude of the simulated trends in these regions (0.8 and 0.6 $\mathrm{W\,m^{-2}\,dec^{-1}}$) are in good agreement with the estimates derived using MODIS surface albedo ($\mathrm{SDRECS_M}$) but significantly lower than those derived from CERES-SYN ($\mathrm{SDRECS_{CS}}$). This discrepancy will be discussed further in section 3.2.1.

Over India, all observation-based estimates of SDRECS exhibit a significant decrease (-1.0 – $-1.9\mathrm{W\,m^{-2}\,dec^{-1}}$), i.e., an increase in the radiation scattered to space by aerosols. Unlike in the US and Europe, the simulated change in SDRECS (-2.4 $\mathrm{W\,m^{-2}\,dec^{-1}}$) is in better agreement with $\mathrm{SDRECS_{CS}}$. Note that changes in -Rsutcs are opposite in sign to those of SDRECS. These contrasting trends will be discussed further in section 3.2.2.

Over Eastern China, observational estimates of SDRECS all show a rapid decrease of SDRECS from 2001 to 2007, followed by an increase until 2015, with no significant trend overall. The timing of the reversal is consistent with previous analysis of changes in AOD (Zhao et al., 2017) and Rsutcs over the China sea (Alfaro-Contreras et al., 2017). AM3 fails to capture this reversal and simulates a significant decrease in SDRECS from 2001 to 2015 (-1.3 $\mathrm{W\,m^{-2}\,dec^{-1}}$). Changes in SDRECS over China will be discussed in section 3.2.3.

3.2.1 Western Europe and Eastern US

Fig. 5 shows the observed and simulated seasonal changes in AOD and SDRECS over Western Europe. The first row shows the speciated AM3 AOD (bars) along with the MODIS TERRA (solid black), MODIS AQUA (cross), and MISR (diamond) AOD. For each season, AM3 is sampled where MODIS TERRA has valid observations for each month in the season. The second row shows the model-derived contribution of individual aerosol types to the overall SDRECS. The bottom row shows the annual anomaly in observation-based and model seasonal SDRECS.

Changes in AOD are dominated by spring and summer, with MODIS TERRA AOD decreasing -0.4 $\mathrm{dec^{-1}}$ in both seasons. Similarly, all estimates of SDRECS show increases of 1 to 1.8 $\mathrm{W\,m^{-2}\,dec^{-1}}$ in spring and 1.2 to 2.5 $\mathrm{W\,m^{-2}\,dec^{-1}}$ in summer (Table 1). These changes are well captured in AM3, where they are driven almost entirely by the decrease of sulfate aerosols associated with declining $\mathrm{SO_2}$ emissions. The slower changes in winter and fall can be attributed to the smaller contribution of sulfate to the aerosol burden and the weaker response of sulfate to declining $\mathrm{SO_2}$ emissions in these seasons (Wang et al., 2011; Paulot et al., 2017a).

Atmos. Chem. Phys. Discuss., https://doi.org/10.5194/acp-2018-148
Manuscript under review for journal Atmos. Chem. Phys.
Discussion started: 13 February 2018

Atmospheric Chemistry and Physics Discussions

Fig. 6 shows the changes in AOD and SDRECS over the Eastern US. The overall pattern is very similar to Western Europe with large reductions in AOD (up to -0.11 dec^{-1}) and increases in SDRECS (up to 3.6 $\mathrm{W\,m^{-2}\,dec^{-1}}$) in spring and summer (Table 1). AM3 underestimates MODIS AOD as well as the rate of change of SDRECS and AOD (from all instruments) in summer (Table 1). This is consistent with the model low bias against $\mathrm{SO_4^{2-}}$ concentration in rain water in the US (Paulot et al., 2016). Similar to observations, AM3 shows greater seasonal contrast between spring and summer in the US than in Europe. In the model, this is driven by more efficient springtime oxidation of $\mathrm{SO_2}$ in Europe, where high emissions of $\mathrm{NH_3}$ facilitate its in-cloud oxidation by ozone.

Note that in both Europe and the US, the magnitude and the trends of the MATCH AOD are greater than for MODIS (collection 6). These differences may be associated with changes in the MODIS AOD retrievals as MATCH uses the older collection 5, and could explain the larger changes in $\mathrm{SDRECS_{CS}}$ relative to $\mathrm{SDRECS_{CE}}$ and $\mathrm{SDRECS_{M}}$ (Table 1).

3.2.2 India

Fig. 7 shows the changes in AOD and SDRECS over India. We will focus here on changes during the winter (DJF) and premonsoon seasons (MAM).

In winter, previous studies have shown that aerosols are primarily of anthropogenic origin (Babu et al., 2013; Pan et al., 2015). During this season, all instruments show a significant increase in AOD (up to 0.13 dec^{-1}). However, we find that the expected increase in Rsutcs is masked by a concomitant darkening of the surface (Table S2), which may be associated with increased leaf area index (LAI, Zhu et al. (2016)). We estimate that SDRECS decreased from 2001 to a 2015 at an average rate of -0.8 – -2.8 $\mathrm{W\,m^{-2}\,dec^{-1}}$. This large range reflects differences between the MODIS and CERES salb products, with MODIS salb showing less rapid darkening.

Table 1 shows that the simulated AOD agrees well for both magnitude and trend with MODIS AOD but overestimates the change in MISR and MATCH AOD. The large difference between MODIS and MATCH AOD may also be associated with changes in LAI as the effect of vegetation on surface reflectivity was revised in collection 6 (Levy et al., 2013b). AM3 falls at the upper end of observational estimates for SDRECS (-2.7 $\mathrm{W\,m^{-2}\,dec^{-1}}$), in good agreement with $\mathrm{SDRECS_{CS}}$ (-2.6 $\mathrm{W\,m^{-2}\,dec^{-1}}$). However, the agreement with $\mathrm{SDRECS_{CS}}$ is fortuitous as the higher surface albedo in AM3 (0.166) relative to CERES-SYN (0.129) tends to dampen changes in aerosol scattering. We calculate that the lower albedo in CERES-SYN would amplify the simulated trend by -0.8 $\mathrm{W\,m^{-2}\,dec^{-1}}$. This suggests that AM3 overestimates the decrease in SDRECS by 1 to 2 $\mathrm{W\,m^{-2}\,dec^{-1}}$.

The model high bias for the rate of change in SDRECS may reflect insufficient aerosol absorption or excessive aerosol scattering. Table 1 shows that black carbon cancels out one third (0.9 $\mathrm{W\,m^{-2}\,dec^{-1}}$) of the decrease in SDRECS, much more than in the US and Europe. This is likely to be an underestimate as the prevalent use of biofuel in winter, a large source of BC (Pan et al.,

Atmos. Chem. Phys. Discuss., https://doi.org/10.5194/acp-2018-148
Manuscript under review for journal Atmos. Chem. Phys.
Discussion started: 13 February 2018

Atmospheric Chemistry and Physics Discussions

2015), is not represented in CMIP6 emission inventory. Table 1 also shows that the increase of nitrate aerosols is the dominant driver for SDRECS change in winter (-2.4 $\mathrm{W\,m^{-2}\,dec^{-1}}$). Nitrate is formed via the reaction of ammonia (primarily from agriculture) and nitric acid (from the oxidation of NO, whose emissions are dominated by fossil fuel combustion). In the CMIP6 emission inventory, the seasonality of ammonia emissions in India follows that of Europe, with a peak in spring. We conducted a sensitivity simulation using the seasonality of $\mathrm{NH_3}$ column from AIRS (Warner et al., 2017) to modulate $\mathrm{NH_3}$ emissions. We find that this revised seasonality significantly reduces the simulated winter trend in SDRECS (0.08 $\mathrm{W\,m^{-2}\,dec^{-1}}$), improving the agreement with observations.

In the premonsoon season, Fig. 7 shows that AOD changes much less rapidly than in winter (Table 1). For instance, MODIS AOD increases by 0.04 $\mathrm{dec^{-1}}$ in MAM, less than a third of the rate in winter. In contrast, AM3 simulates an increase in AOD of 0.15 $\mathrm{dec^{-1}}$, similar to the rate of change in winter (Table 1). We also find a significant decrease (-0.07 $\mathrm{dec^{-1}}$) in the MODIS-derived dust optical depth (Ginoux et al., 2012), consistent with the decline in coarse-mode aerosols in the Indo-Gangetic Plain (IGP, Babu et al. (2013)). This decline of dust is not captured by AM3 and could account for most of the discrepancy between model and simulated AOD trends. Such decrease in dust would also reduce the magnitude of the change in SDRECS from -3.1 to -1.7 $\mathrm{W\,m^{-2}\,dec^{-1}}$, in better agreement with the observation-based range of -0.9 – -1.4 $\mathrm{W\,m^{-2}\,dec^{-1}}$. To our knowledge, the mechanism for this decrease of dust over India in spring has not been identified. Babu et al. (2013) reported that the GOCART model, which uses the same dust emission parameterization as AM3 (Ginoux et al., 2001), but includes modulation of soil bareness by vegetation (Kim et al., 2013), does exhibit a decrease in the dust burden in the IGP. More studies are clearly needed to better understand the cause of the LAI increase in India and its connection with surface darkening and the decrease of spring dust, as both these processes have masked the impact of anthropogenic aerosols on the outgoing shortwave radiation.

3.2.3 Eastern China

Fig. 8 shows the change in AOD and SDRECS over Eastern China. AM3 captures the average magnitude of AOD well in winter and spring but underestimates AOD (MODIS) during the monsoon and post monsoon seasons. Although there are significant differences between the different AOD retrievals (Zhao et al., 2017), no homogeneous trend is detected in either AOD or SDRECS over the 2001-2015 period in any season. Note that recent studies show that MODIS AOD is biased high against ground-based observations in China (Tao et al., 2015; Xiao et al., 2016), which may be associated with the representation of surface properties in the retrieval algorithm (Wu et al., 2016).

In contrast to observations, AM3 exhibits a large positive trend in AOD and negative trend in SDRECS in spring (0.15 $\mathrm{dec^{-1}}$ and -2.1 $\mathrm{W\,m^{-2}\,dec^{-1}}$, respectively) and summer (0.11 $\mathrm{dec^{-1}}$ and -1 $\mathrm{W\,m^{-2}\,dec^{-1}}$, respectively). Changes are greatest in spring, when large emissions of $\mathrm{NH_3}$ favor both the production of nitrate and sulfate (via in-cloud oxidation by ozone) aerosols. Sulfate is the

Atmos. Chem. Phys. Discuss., https://doi.org/10.5194/acp-2018-148
Manuscript under review for journal Atmos. Chem. Phys.
Discussion started: 13 February 2018

Atmospheric Chemistry and Physics Discussions

largest contributor to the AOD and SDRECS in spring, but changes are dominated by the increase of nitrate aerosols (0.08 dec^{-1} and -2.2 $\mathrm{W\,m^{-2}\,dec^{-1}}$, respectively Table 1).

Similar to India, this model bias may be associated with uncertainties in anthropogenic emissions. Fig. 1 shows that Chinese SO_2 emissions in the CMIP6 emission inventory are nearly stable after 2007, while NO and BC emissions increase until 2013 before stabilizing. In contrast, the Modular Emission Inventory for China (MEIC), a regional inventory, designed to take into account the impact of rapid technological and regulatory changes on emissions (Zhang et al., 2009), shows a decline of SO_2 emissions starting in 2006 and accelerating in 2012, a decrease of NO after 2012, and near-stable BC emissions after 2007. In 2014, MEIC NO, SO_2, and BC emissions are 24%, 48%, and 32% lower than CMIP6 emissions, respectively. NH_3 emissions are similar in magnitude but exhibit different seasonality. CMIP6 NH_3 emissions peak in spring, while MEIC exhibits a broad peak in summer, which is supported by top-down constraints (Paulot et al., 2014; Zhang et al., 2017). A detailed evaluation of these two emission inventories is beyond the scope of this study. However, observations show significant declines in SO_2 columns starting in 2008 (Li et al., 2010; Irie et al., 2016; de Foy et al., 2016; Liu et al., 2016; Ding et al., 2017; van der A et al., 2017; Krotkov et al., 2016) and NO_2 starting in 2012 (Liu et al., 2016; van der A et al., 2017), which is consistent with MEIC trends. We refer the reader to the recent study of van der A et al. (2017) for a detailed discussion of the technological and regulatory changes that have contributed to the changes in Chinese emissions over the 2001-2015 period.

In order to assess the impact of these revised emissions on the simulated AOD and SDRECS, we perform a sensitivity simulations using MEIC BC, SO_2, NH_3 and NO emissions for China (Fig. S1). We find that MEIC emissions reduce the simulated AOD trend by 40% in spring primarily through reduction in sulfate aerosols. The change in the SDRECS trend is smaller (-15%) as opposite changes in SDRECS(BC) and SDRECS(SUL) offset each other. This small reduction does not improve the simulated annual trend (-1.8 $\mathrm{W\,m^{-2}\,dec^{-1}}$), as higher emissions of ammonia in winter and fall result in higher sulfate and nitrate in these seasons, in spite of lower NO and SO_2 emissions.

The lack of sensitivity of sulfate to SO_2 emissions reflects strong oxidant limitations in AM3 (Paulot et al., 2017a). However, recent studies have shown that the oxidation pathways of SO_2 represented in AM3, e.g., homogeneous oxidation by OH and aqueous oxidation by O_3 and H_2O_2, can not sustain the observed concentrations of sulfate in the North China Plains (Wang et al., 2014a; Zheng et al., 2015). Under hazy conditions, heterogeneous oxidation of SO_2 by NO_2 (Cheng et al., 2016) or O_2 (Hung and Hoffmann, 2015) at the surface of or in aerosols may be the dominant sources of SO_4^{2-}, although the relative importance of these pathways remains uncertain (Guo et al., 2017; He et al., 2017). In order to quantify the sensitivity of our results to these reactions, we perform an additional simulation using the parameterization of the uptake coefficient of SO_2 on aerosols derived by Zheng et al. (2015):

Atmos. Chem. Phys. Discuss., https://doi.org/10.5194/acp-2018-148
Manuscript under review for journal Atmos. Chem. Phys.
Discussion started: 13 February 2018

Fig. 9 shows that the heterogeneous oxidation of SO_2 increases the simulated sulfate optical depth by 100% in winter and 62% in fall. Changes are much smaller ($< 25\%$) in spring and summer, because of greater oxidant availability. The increased production of sulfate in winter and fall results in a stronger link between SO_2 emissions and simulated AOD and SDRCES. This allows the model to better capture some prominent features in the observational record, such as the SDRECS dip and AOD peak in fall 2006, as well as the decrease in AOD and increase in SDRECS after 2013. However, on an annual basis, the simulated decrease in SDRECS remains biased high relative to observations, as AM3 does not capture the increase in SDRECS from 2007 to 2015 (not shown).

4 Implication for the aerosol direct forcing

The aerosol direct forcing (DRF, Heald et al. (2014)) is a measure of the change in DRE associated with anthropogenic emissions since preindustrial time (taken here as 1850). In section 3.2, we have shown that regional differences in the speciation of anthropogenic emissions and the oxidative environment are important to understand changes in SDRECS over the largest sources of anthropogenic pollution. Here, we examine whether these changes have changed the sensitivity of DRF to anthropogenic emissions.

To examine this issue, we compare changes in simulated all-sky and clear-sky direct radiative forcing (DRF and DRFCS, respectively) for two time periods, 1850 to 2001 and 2001 to 2015. We estimate the DRF for 2001 and 2015 as

$$DRF(y) = DRE(anthro = y, met = y) - DRE(anthro = 1850, met = y) \quad (3)$$

where $anthro$ and met denote the year used for anthropogenic emissions and to nudge the horizontal wind, respectively. Note that we use the same meteorology for both simulations, in order to minimize differences in natural sources (e.g., dust, dimethylsulfide). Following the AEROCOM practice (Myhre et al., 2013), we do not consider biomass burning as part of the anthropogenic emissions. On the basis of our evaluation of AM3, we include MEIC emissions for China, revised NH_3 seasonality in India, and the heterogeneous oxidation of SO_2 on aerosol surfaces.

Fig. 10 (panels a and b) shows the meridional changes in anthropogenic emissions of BC, NO, NH_3 and SO_2 between 1850 and 2001 (a) and 2001 and 2015 (b). The overall change in BC, NO, and NH_3 from 2001 to 2015 are 25%, 15%, and 19% of their change from 1850 to 2001. In contrast, SO_2 emissions have been reduced by 12.5%. From 2001 to 2015, BC and NH_3 have increased in most regions, while both SO_2 and NO emissions have declined in the northern midlatitudes but increased in the tropics.

Changes in the DRFCS (Fig. 10c) of individual aerosols from 1850 to 2001 largely mirror the emissions of their precursors. Some deviations can be noted however. For instance, DRFCS(BC) is enhanced at high latitudes because of high surface albedo (Myhre et al., 2013)), while the broader

Atmos. Chem. Phys. Discuss., https://doi.org/10.5194/acp-2018-148
Manuscript under review for journal Atmos. Chem. Phys.
Discussion started: 13 February 2018

Atmospheric Chemistry and Physics Discussions

latitudinal extend of DRFCS(SUL) relative to SO_2 emissions is partly associated with the less efficient oxidation of SO_2 over large source regions (Fig. S2).

The overall DRFCS decreases by -0.64 $\mathrm{W\,m^{-2}}$ from 1850 to 2001, which agrees well with previous assessments (Table S3). Changes in DRFCS reflect the competing effects of changes in SO_4^{2-} (DRFCS(SUL) = -0.73 $\mathrm{W\,m^{-2}}$) and BC (DRFCS(BC)=0.36 $\mathrm{W\,m^{-2}}$). DRFCS changes little between 2001 and 2015 (-0.04 $\mathrm{W\,m^{-2}}$) consistent with previous studies (Murphy, 2013; Kühn et al., 2014). In AM3, this reflects the near cancellation between the increase in DRFCS in the northern midlatitudes (associated with the decrease of sulfate and the increase of BC) and the decrease of DRFCS in the northern tropics (associated with the increase of nitrate and sulfate aerosols).

The change of DRFCS(BC) from 2001 to 2015 is 25% of the change from 1850 to 2001, in good agreement with the change in BC emissions. In contrast, the relationship between DRFCS(SUL) (+3%) and changes in SO_2 emissions (-12.5%) is different from the 1850–2001 period. This primarily reflects regional differences in the oxidative environment (Fig. S2), with greater conversion efficiency of SO_2 to SO_4^{2-} in the tropics, where SO_2 emissions increase, than in the midlatitudes, where they decrease. Furthermore, the fraction of SO_2 molecules oxidized to SO_4^{2-} tends to increase with decreasing SO_2 emissions, as oxidant limitations become less important. This tends to dampen the response of DRFCS(SUL) to the decrease of SO_2 emissions in the midlatitudes (Paulot et al., 2017a). Similar to sulfate, the change in DRFCS(NIT) (+75%) is different from the changes in the emissions of nitrate precursors (NH_3 and NO emissions increase by less than 20%). This higher sensitivity reflects in part the decrease of sulfate in the northern midlatitudes, which enables more ammonia to react with nitric acid to produce ammonium nitrate (Ansari and Pandis, 1998). In addition, the magnitudes of both DRFCS(NIT) and DRFCS(SUL) increase in the tropics, which reflects the higher ratio of NH_3 to SO_2 emissions in this region.

Clouds can enhance the reflectivity of the surface beneath aerosols as well as mask the effect of aerosols underneath (Heald et al., 2014). Overall clouds tend to amplify the forcing of absorbing aerosols and diminish that of scattering aerosols. The simulated DRF(2001) is -0.09 $\mathrm{W\,m^{-2}}$, at the low end of previous multi-model assessments (Table S2) switching sign from negative to positive North of 45°. For comparison, the instantaneous radiative forcing from well-mixed greenhouse gases at TOA, as calculated from the GFDL Standalone radiation code (Schwarzkopf and Ramaswamy, 1999; Freidenreich and Ramaswamy, 1999), is 1.84 $\mathrm{W\,m^{-2}}$ in 2001. From 2001 to 2015, DRF is simulated to increase by 0.03 $\mathrm{W\,m^{-2}}$ and 0.27 $\mathrm{W\,m^{-2}}$ from aerosols and well-mixed greenhouse gases, respectively. In the northern midlatitudes, the decrease of sulfate and the increase in black carbon are simulated to increase the regional direct radiative forcing by up to 0.25 $\mathrm{W\,m^{-2}}$, which is comparable to the forcing from greenhouse gases. This highlights the need to account for aerosols to characterize recent regional changes in radiative forcing.

Atmos. Chem. Phys. Discuss., https://doi.org/10.5194/acp-2018-148
Manuscript under review for journal Atmos. Chem. Phys.
Discussion started: 13 February 2018

Atmospheric Chemistry and Physics Discussions

5 Conclusions

We have used observations of the outgoing shortwave radiation and the variability in surface albedo, ozone, and water vapor to estimate changes in the aerosol shortwave direct effect under clear sky (SDRECS) from 2001 to 2015.

We use these observational constraints over large source regions of pollution to evaluate the representation of anthropogenic emissions and their impact on atmospheric chemistry and radiative forcing in the GFDL-AM3 chemistry climate model. Our work suggests a mature understanding of changes in the US and Europe, which are dominated by the ongoing decrease of SO_2 sources. In contrast, the different mix of anthropogenic emissions in India and China results in a more complex speciation of SDRECS, with large contributions from sulfate, nitrate, and black carbon. These regions remain challenging to capture in AM3. First, we find significant uncertainties in the CMIP6 emissions, including in the seasonality of NH_3, which is based on agricultural practices in Europe, and in the seasonality of black carbon, which is neglected in India. The reduction of Chinese anthropogenic emissions of SO_2 and NO after 2007 is also underestimated and results in an excessive decrease in SDRECS over China and the Western Pacific. Second, differences in regional photochemistry result in different sensitivity of SDRECS to anthropogenic emissions in China and India compared to the Eastern US and Europe. In particular, the competition for ammonia between sulfate and nitrate tends to limit the formation of nitrate in the US and Europe. In contrast, in India, larger emissions of both ammonia and nitrogen oxide enables both sulfate and nitrate to increase from 2001 to 2015. In addition, we find that the model better captures the variability in SDRECS over China, when accounting for the heterogeneous oxidation of SO_2 on aerosols, a reaction that has little impact on the sulfate budget in Europe and the US.

We find that even over regions of high anthropogenic emissions, changes in Rsutcs are not necessarily associated with changes in anthropogenic aerosols. In particular, in India, a darkening of the surface, possibly associated with an increase in LAI, and a decline in dust sources may have masked much the anthropogenic signal in Rsutcs over the 2001-2015 period.

Clearly more work is needed to further characterize the regional speciation of SDRECS and its sensitivity to changes in anthropogenic emissions. In particular, we have shown that it is important to account for changes in the ratio of SO_2 to BC emissions and for non-linearities in nitrate and sulfate chemistry to understand recent changes in DRF. Therefore, attempts to describe DRF, simply as a function of SO_2 (Stevens and Schwartz, 2012) need to be revisited (Stevens et al., 2017).

Acknowledgements. We thank the many researchers, who have contributed to the CERES, MODIS, and MISR products used in this study. CERES data were obtained from the NASA Langley Research Center CERES ordering tool at http://ceres.larc.nasa.gov/. MODIS albedo (MD43C3 MODIS/Terra+Aqua BRDF/Albedo Albedo Daily L3 Global 0.05 Deg CMG V006) was obtained in netCDF file format from the Integrated Climate Data Center (ICDC, http://icdc.cen.uni-hamburg.de, University of Hamburg, Hamburg, Germany). MISR and MODIS AOD products can be obtained from the NASA Earthdata portal. Model outputs are available upon request to Fabien.Paulot@noaa.gov. We thank Drs Bo Zheng and Qiang Zhang for providing MEIC gridded emissions. This work was supported by NOAA Climate Program Office. P. G. acknowledges partial funding by NASA through NNH14ZDA001N-ACMAP grant. We thanks A. Jones and L. J. Donner for helpful comments.

Atmos. Chem. Phys. Discuss., https://doi.org/10.5194/acp-2018-148
Manuscript under review for journal Atmos. Chem. Phys.
Discussion started: 13 February 2018

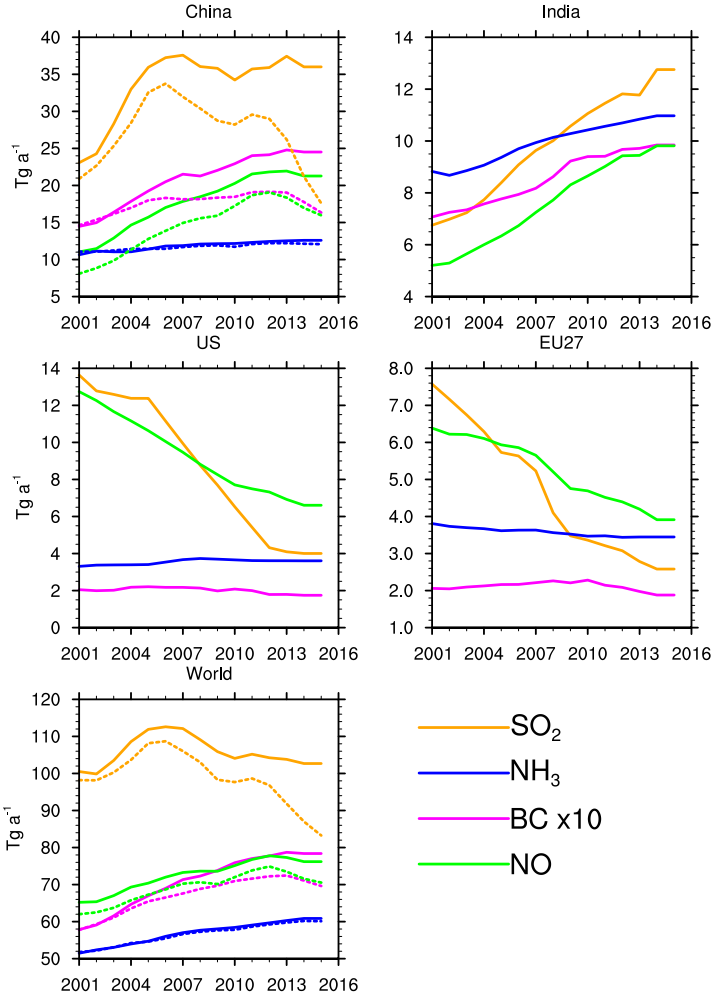

Figure 1. Annual anthropogenic emissions of SO_2, BC, NH_3, and NO from CEDS (solid lines) in selected regions. Emissions of SO_2, and NO with anthropogenic emissions from MEIC (for agriculture, energy, transportation, industry, and residential sectors) are also shown (dash lines).

Atmos. Chem. Phys. Discuss., https://doi.org/10.5194/acp-2018-148
Manuscript under review for journal Atmos. Chem. Phys.
Discussion started: 13 February 2018

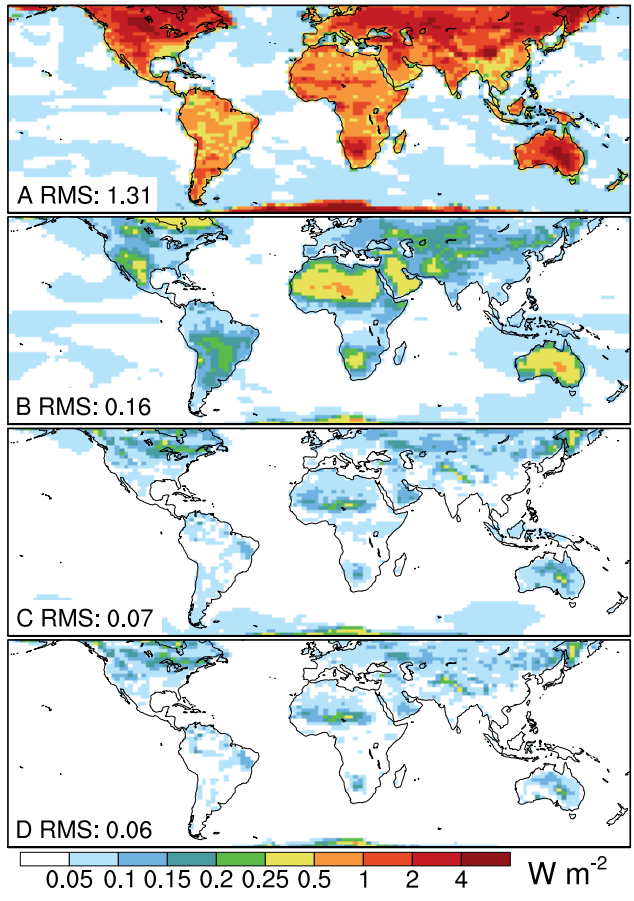

Figure 2. Root mean square of the annual anomaly in the outgoing clear-sky shortwave radiation without aerosols (Rsutcsaf) and its decrease after accounting for the effect of albedo (B), albedo and water vapor (C), albedo, water vapor, and ozone (D), as described in equation 2. The area weighted RMS over land from 60S to 60N is in indicated in each panel

Atmos. Chem. Phys. Discuss., https://doi.org/10.5194/acp-2018-148
Manuscript under review for journal Atmos. Chem. Phys.
Discussion started: 13 February 2018

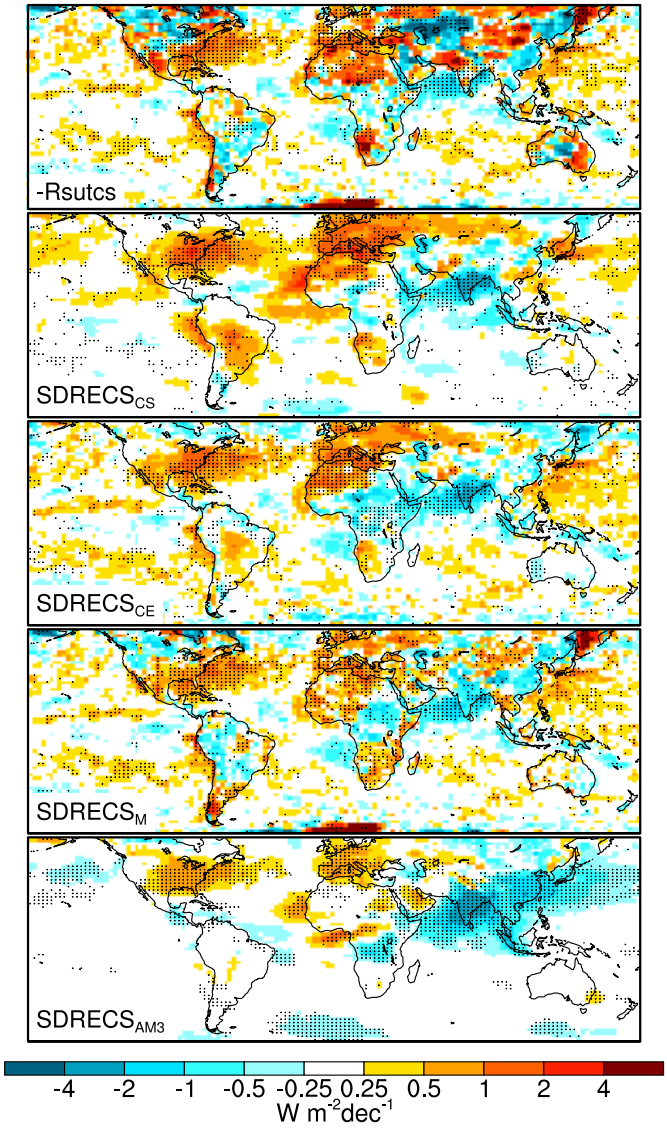

Figure 3. Decadal rate of change in the aerosol shortwave direct effect under clear sky (SDRECS). An increase in SDRECS reflects a decrease in the amount of radiation scattered to space by aerosols. The CERES SYN estimate ($\mathrm{SDRECS_{CS}}$) is based on calculated clear-sky outgoing shortwave fluxes with and without aerosols, constrained by observations. $\mathrm{SDRECS_{CE}}$ and $\mathrm{SDRECS_{M}}$ are estimated using the observed clear-sky outgoing shortwave fluxes from CERES EBAF, water vapor and ozone from GEOS 5, and the surface albedo from CERES-EBAF and MODIS, respectively. The bottom panel shows the simulated change in SDRECS by the GFDL AM3 model ($\mathrm{SDRECS_{AM3}}$). The top panel shows the change in outgoing shortwave radiation Rsutcs (plotted as -Rsutcs for consistency with the definition of SDRECS). Dotted areas are significant at the 95% confidence level.

Atmos. Chem. Phys. Discuss., https://doi.org/10.5194/acp-2018-148
Manuscript under review for journal Atmos. Chem. Phys.
Discussion started: 13 February 2018

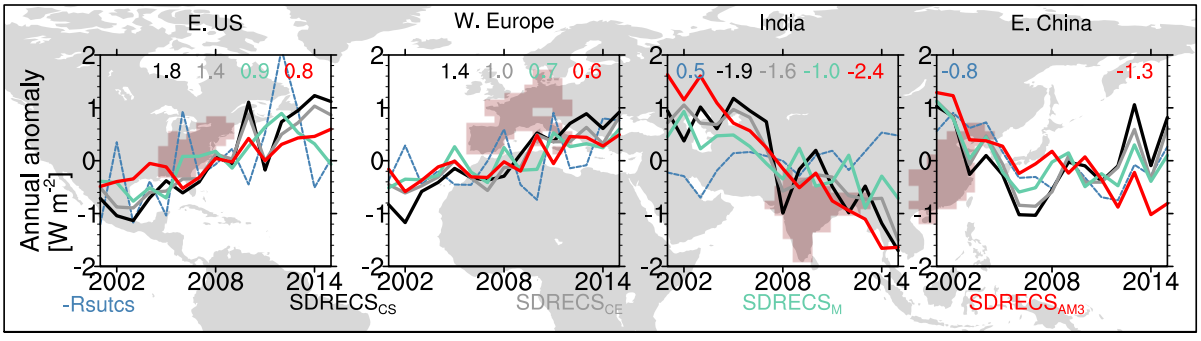

Figure 4. Regional changes in the annual anomaly of the aerosol shortwave direct effect under clear sky (from CERES-SYN ($\mathrm{SDRECS_{CS}}$, black), and from CERES-EBAF corrected using CERES ($\mathrm{SDRECS_{CE}}$, grey), and MODIS ($\mathrm{SDRECS_{M}}$) surface albedo) over the Eastern US, Western Europe, India, and Eastern China. The simulated annual anomaly in $\mathrm{SDRECS_{AM3}}$ and in the outgoing shortwave radiation Rsutcs (plotted as -Rsutcs for consistency with the definition of SDRECS) are shown in red and blue, respectively. The magnitude of the linear decadal trend of each timeseries (in $\mathrm{W\,m^{-2}\,dec^{-1}}$) is indicated in inset when the trend is significant at p=0.05.

Atmos. Chem. Phys. Discuss., https://doi.org/10.5194/acp-2018-148
Manuscript under review for journal Atmos. Chem. Phys.
Discussion started: 13 February 2018

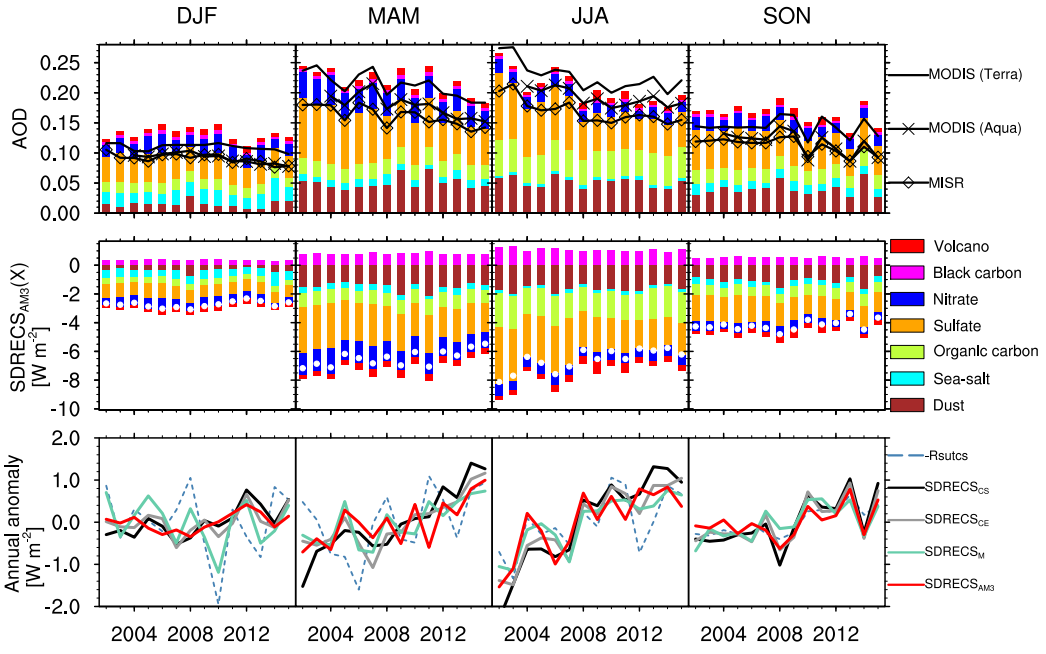

Figure 5. Seasonal changes in AOD and SDRECS in Western Europe (Fig. 4). The top row shows the observed aerosol optical depth from different space-borne platforms (MODIS-Terra (lines), MODIS-Aqua (cross), MISR (diamond)) and the simulated model AOD decomposed into its components (bars). The second row shows the individual aerosol SDRECS and the net SDRECS (white circle). The bottom row shows the observed and simulated seasonal anomalies in SDRECS (solid lines) and -Rstucs (dash blue line).

Atmos. Chem. Phys. Discuss., https://doi.org/10.5194/acp-2018-148
Manuscript under review for journal Atmos. Chem. Phys.
Discussion started: 13 February 2018

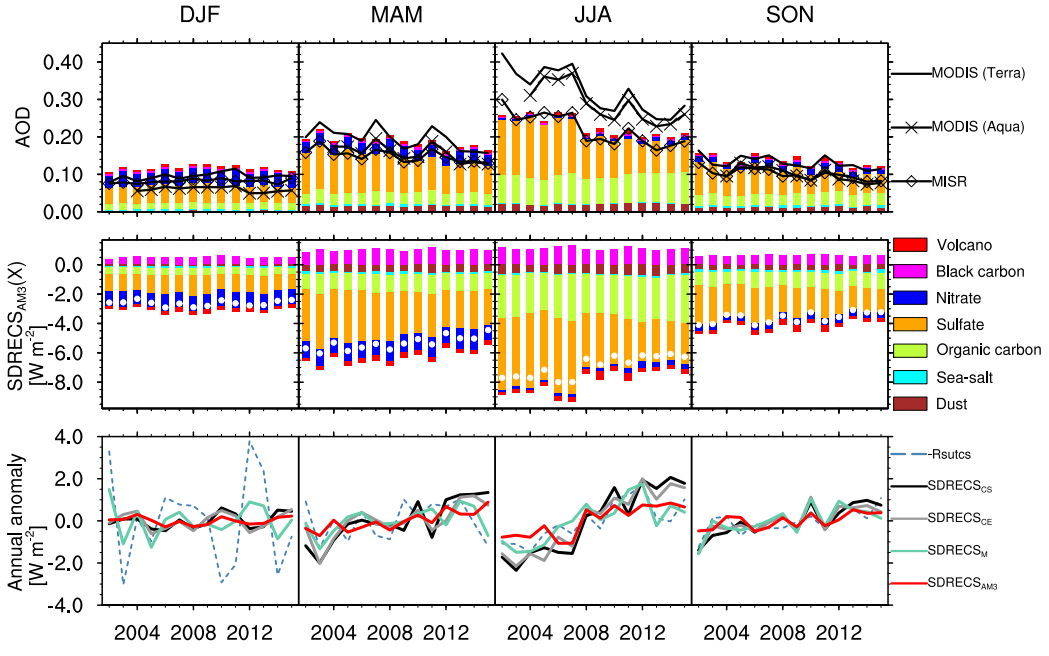

Figure 6. Same as 5 for the Eastern US

Atmos. Chem. Phys. Discuss., https://doi.org/10.5194/acp-2018-148
Manuscript under review for journal Atmos. Chem. Phys.
Discussion started: 13 February 2018

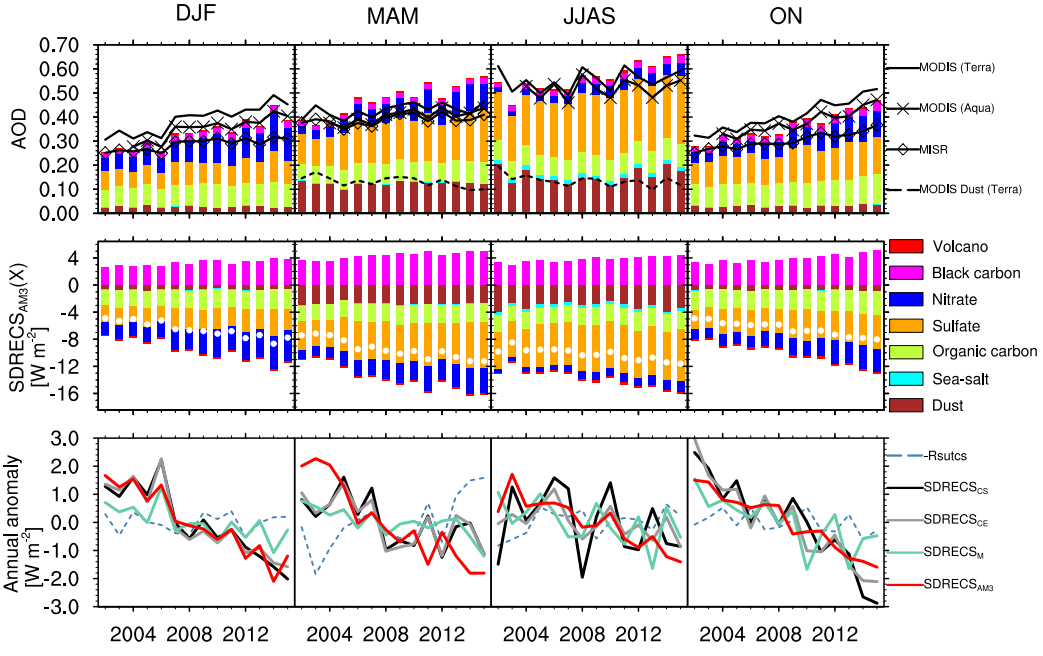

Figure 7. Same as 5 for the India. MISR is excluded in the monsoon season, when its coverage is too sparse relative to MODIS (TERRA).

Atmos. Chem. Phys. Discuss., https://doi.org/10.5194/acp-2018-148
Manuscript under review for journal Atmos. Chem. Phys.
Discussion started: 13 February 2018

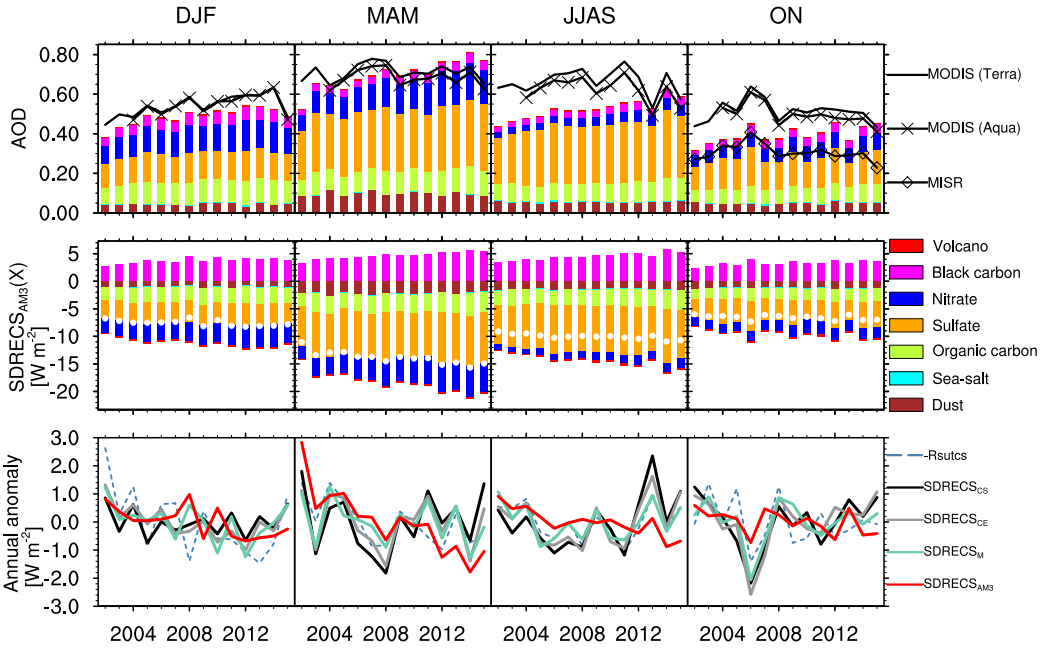

Figure 8. Same as 5 for Eastern China. MISR is excluded in winter, spring, and monsoon seasons, when its coverage is too sparse.

Atmos. Chem. Phys. Discuss., https://doi.org/10.5194/acp-2018-148
Manuscript under review for journal Atmos. Chem. Phys.
Discussion started: 13 February 2018

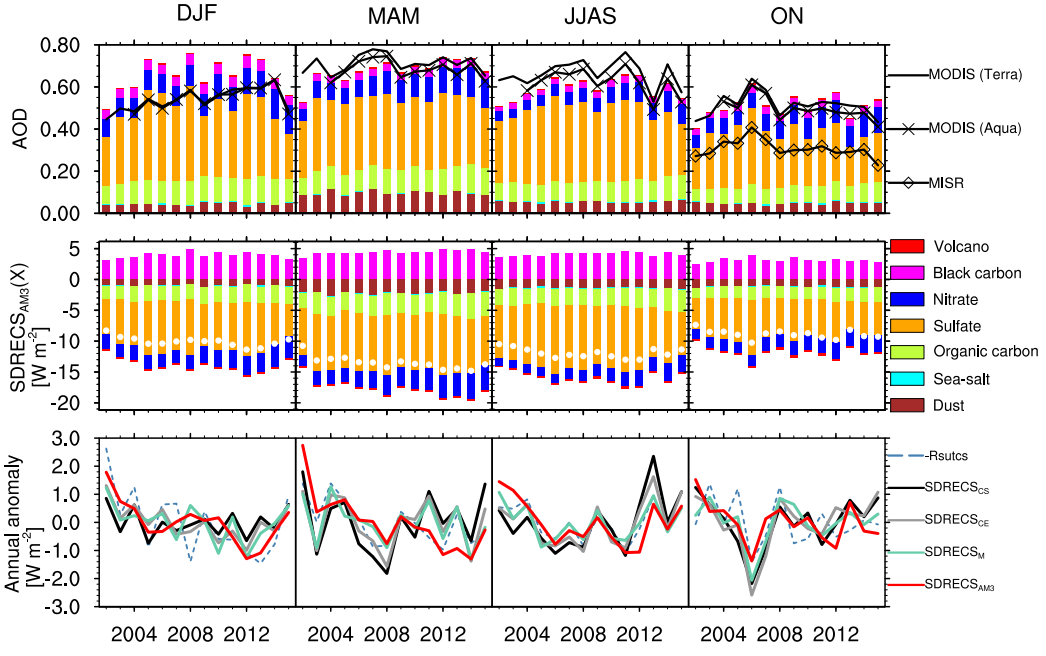

Figure 9. same as Fig. 8 but with MEIC SO_2 and NO emissions, revised NH_3 seasonality, and heterogeneous oxidation of SO_2 (see text)

Atmos. Chem. Phys. Discuss., https://doi.org/10.5194/acp-2018-148
Manuscript under review for journal Atmos. Chem. Phys.
Discussion started: 13 February 2018

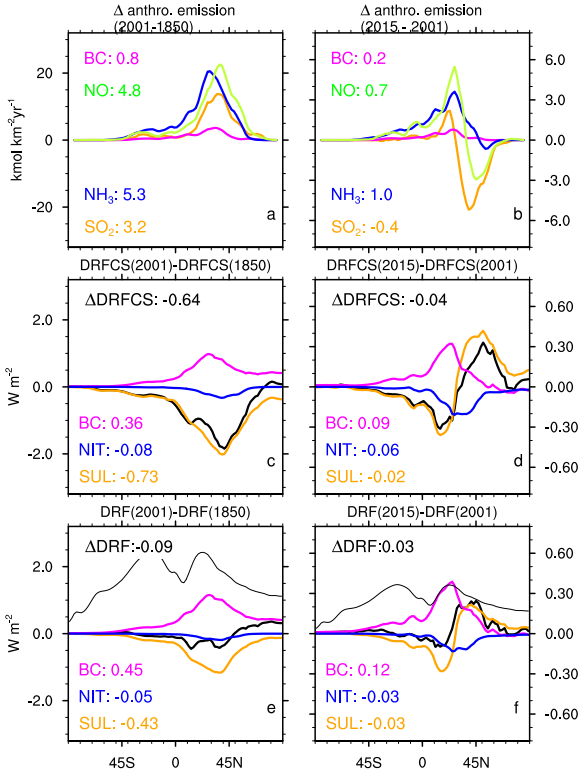

Figure 10. Meridional distribution of changes in anthropogenic emissions (BC, NO, NH_3, and SO_2) and in clear-sky (DRFCS, middle row) and all-sky radiative aerosol direct radiative forcing (DRF, bottom row) from 1850 to 2001 (left) and from 2001 to 2015 (right). The thin black line indicates the instantaneous radiative forcing at TOA from well-mixed greenhouse gases. Global anthropogenic emissions and the total and speciated DRFCS and DRF are indicated inline.

Atmos. Chem. Phys. Discuss., https://doi.org/10.5194/acp-2018-148
Manuscript under review for journal Atmos. Chem. Phys.
Discussion started: 13 February 2018

Atmospheric Chemistry and Physics Discussions

Table 1. Observation-based estimates and simulated decadal trends in AOD, SDRECS ($\mathrm{W\,m^{-2}\,dec^{-1}}$) for selected regions and seasons from 2002 to 2015[a]

	Western Europe		Eastern US		India		Eastern China
	MAM	JJA	MAM	JJA	DJF	MAM	MAM
AOD							
MODIS (TERRA)	-0.04 [0.21]	-0.04 [0.23]	-0.04 [0.20]	-0.11 [0.32]	0.13 [0.39]	0.04 [0.43]	* [0.71]
MODIS (AQUA)	-0.05 [0.18]	-0.03 [0.19]	-0.04 [0.16]	-0.10 [0.29]	0.11 [0.35]	0.07 [0.40]	* [0.68]
MISR	-0.03 [0.16]	-0.03 [0.17]	-0.02 [0.15]	-0.08 [0.22]	0.05 [0.29]	* [0.39]	
MATCH[b]	-0.06 [0.27]	-0.06 [0.26]	-0.07 [0.29]	-0.11 [0.35]	0.03 [0.49]	* [0.64]	* [0.90]
AM3	-0.04 [0.22]	-0.05 [0.21]	-0.03 [0.19]	-0.05 [0.23]	0.13 [0.33]	0.15 [0.47]	0.15 [0.70]
SUL	-0.03 [0.08]	-0.04 [0.07]	-0.03 [0.09]	-0.06 [0.12]	0.02 [0.09]	0.07 [0.17]	0.05 [0.30]
NIT	-0.01 [0.04]	* [0.02]	* [0.03]	0.00 [0.01]	0.07 [0.10]	0.06 [0.07]	0.08 [0.14]
BC	* [0.01]	* [0.00]	* [0.01]	* [0.00]	0.01 [0.02]	0.01 [0.02]	0.01 [0.04]
SDRECS							
CS	1.8 [-8.9]	2.5 [-9.4]	2.1 [-8.6]	3.6 [-11.0]	-2.6 [-9.1]	-1.4 [-13.4]	* [-20.5]
CE	1.4	1.8	1.4	3.4	-2.3	-1.2	*
M	1.0	1.2	*	2.0	-0.8	-0.9	*
AM3	1.1 [-6.5]	1.5 [-6.6]	0.9 [-5.3]	1.4 [-6.9]	-2.7 [-6.6]	-3.1 [-9.4]	-2.1 [-13.9]
SUL	0.9 [-2.6]	1.5 [-2.7]	1.1 [-3.1]	2.2 [-3.9]	-0.7 [-2.9]	-1.8 [-5.5]	-1.1 [-8.5]
NIT	0.3 [-1.4]	* [-0.7]	* [-1.2]	-0.2 [-0.2]	-2.4 [-3.3]	-1.9 [-2.6]	-2.2 [-4.2]
BC	* [0.8]	-0.2 [1.1]	* [1.0]	* [1.1]	0.9 [3.2]	1.2 [4.3]	1.4 [4.7]

[a] The average over the period 2002–2015 is shown in bracket (2003-2015 for AQUA). Trend is estimated using the Theil-Sen method. * denotes non significant monotonous change at p=0.05. Model AOD is sampled based on MODIS (TERRA) seasonal coverage. No statistics is provided for China from MISR because of large differences in spatial coverage with MODIS (TERRA). CS, CE, and M refer to CERES-SYN, CERES-EBAF, and MODIS based estimates, respectively

[b] from CERES-SYN Ed4 based on assimilation of MODIS Collection5 AOD with the MATCH model. Albedo trends are multiplied by 10 for readability

[c] Cloud-free, aerosol-free broadband albedo, except for CE (cloud-free)

References

Alfaro-Contreras, R., Zhang, J., Reid, J. S., and Christopher, S.: A Study of the Longer Term Variation of Aerosol Optical Thickness and Direct Shortwave Aerosol Radiative Effect Trends Using MODIS and CERES, Atmos. Chem. Phys. Discuss., 2017, 1–63, doi:10.5194/acp-2017-365, https://www.atmos-chem-phys-discuss.net/acp-2017-365/, 2017.

Ansari, A. S. and Pandis, S. N.: Response of Inorganic PM to Precursor Concentrations, Environ. Sci. Technol., 32, 2706–2714, 1998.

Babu, S. S., Manoj, M. R., Moorthy, K. K., Gogoi, M. M., Nair, V. S., Kompalli, S. K., Satheesh, S. K., Niranjan, K., Ramagopal, K., Bhuyan, P. K., and Singh, D.: Trends in aerosol optical depth over Indian region: Potential causes and impact indicators, Journal of Geophysical Research: Atmospheres, 118, 2013JD020 507, doi:10.1002/2013JD020507, http://onlinelibrary.wiley.com/doi/10.1002/2013JD020507/abstract, 2013.

Bellouin, N., Boucher, O., Haywood, J., and Reddy, M. S.: Global estimate of aerosol direct radiative forcing from satellite measurements, Nature, 438, 1138–1141, doi:10.1038/nature04348, https://doi.org/10.1038/nature04348, 2005.

Bellouin, N., Jones, A., Haywood, J., and Christopher, S. A.: Updated estimate of aerosol direct radiative forcing from satellite observations and comparison against the Hadley Centre climate model, Journal of Geophysical Research: Atmospheres, 113, n/a–n/a, doi:10.1029/2007JD009385, http://dx.doi.org/10.1029/2007JD009385, d10205, 2008.

Bollasina, M. A., Ming, Y., and Ramaswamy, V.: Anthropogenic Aerosols and the Weakening of the South Asian Summer Monsoon, Science, 334, 502–505, doi:10.1126/science.1204994, http://science.sciencemag.org/content/334/6055/502, 2011.

Boucher, O., Randall, D., Artaxo, P., Bretherton, C., Feingold, G., Forster, P., Kerminen, V.-M., Kondo, Y., Liao, H., Lohmann, U., Rasch, P., Satheesh, S., Sherwood, S., Stevens, B., and Zhang, X.: Clouds and Aerosols, book section 7, pp. 571–658, Cambridge University Press, Cambridge, United Kingdom and New York, NY, USA, doi:10.1017/CBO9781107415324.016, www.climatechange2013.org, 2013.

CERES: CERES EBAF Ed4.0 Data Quality Summary, NASA, https://ceres.larc.nasa.gov/documents/DQ_summaries/CERES_EBAF_Ed4.0_DQS.pdf, 2017.

Cescatti, A., Marcolla, B., Santhana Vannan, S. K., Pan, J. Y., Román, M. O., Yang, X., Ciais, P., Cook, R. B., Law, B. E., Matteucci, G., Migliavacca, M., Moors, E., Richardson, A. D., Seufert, G., and Schaaf, C. B.: Intercomparison of MODIS albedo retrievals and in situ measurements across the global FLUXNET network, Remote Sensing of Environment, 121, 323–334, doi:10.1016/j.rse.2012.02.019, http://www.sciencedirect.com/science/article/pii/S0034425712001125, 2012.

Charlson, R. J., Schwartz, S. E., Hales, J. M., Cess, R. D., Coakley, J. A., Hansen, J. E., and Hofmann, D. J.: Climate Forcing by Anthropogenic Aerosols, Science, 255, 423–430, doi:10.1126/science.255.5043.423, http://science.sciencemag.org/content/255/5043/423, 1992.

Cheng, Y., Zheng, G., Wei, C., Mu, Q., Zheng, B., Wang, Z., Gao, M., Zhang, Q., He, K., Carmichael, G., schl, U. P., and Su, H.: Reactive nitrogen chemistry in aerosol water as a source of sulfate during haze events in China, Science Advances, 2, e1601 530–e1601 530, doi:10.1126/sciadv.1601530, https://doi.org/10.1126/sciadv.1601530, 2016.

Christopher, S. A. and Zhang, J.: Cloud-free shortwave aerosol radiative effect over oceans: Strategies for identifying anthropogenic forcing from Terra satellite measurements, Geophysical Research Letters, 31, n/a–n/a, doi:10.1029/2004GL020510, http://dx.doi.org/10.1029/2004GL020510, l18101, 2004.

Collins, W. D., Rasch, P. J., Eaton, B. E., Khattatov, B. V., Lamarque, J.-F., and Zender, C. S.: Simulating aerosols using a chemical transport model with assimilation of satellite aerosol retrievals: Methodology for INDOEX, Journal of Geophysical Research: Atmospheres, 106, 7313–7336, doi:10.1029/2000JD900507, http://onlinelibrary.wiley.com/doi/10.1029/2000JD900507/abstract, 2001.

de Foy, B., Lu, Z., and Streets, D. G.: Satellite NO2 retrievals suggest China has exceeded its NOx reduction goals from the twelfth Five-Year Plan, Scientific Reports, 6, doi:10.1038/srep35912, https://www.ncbi.nlm.nih.gov/pmc/articles/PMC5082360/, 2016.

Dentener, F., Kinne, S., Bond, T., Boucher, O., Cofala, J., Generoso, S., Ginoux, P., Gong, S., Hoelzemann, J. J., Ito, A., Marelli, L., Penner, J. E., Putaud, J.-P., Textor, C., Schulz, M., van der Werf, G. R., and Wilson, J.: Emissions of primary aerosol and precursor gases in the years 2000 and 1750 prescribed data-sets for AeroCom, Atmospheric Chemistry and Physics, 6, 4321–4344, doi:10.5194/acp-6-4321-2006, https://doi.org/10.5194/acp-6-4321-2006, 2006.

Ding, J., Miyazaki, K., van der A, R. J., Mijling, B., Kurokawa, J.-I., Cho, S., Janssens-Maenhout, G., Zhang, Q., Liu, F., and Levelt, P. F.: Intercomparison of NOx emission inventories over East Asia, Atmos. Chem. Phys., 17, 10 125–10 141, doi:10.5194/acp-17-10125-2017, https://www.atmos-chem-phys.net/17/10125/2017/, 2017.

Donner, L. J., Wyman, B. L., Hemler, R. S., Horowitz, L. W., Ming, Y., Zhao, M., Golaz, J.-C., Ginoux, P., Lin, S.-J., Schwarzkopf, M. D., Austin, J., Alaka, G., Cooke, W. F., Delworth, T. L., Freidenreich, S. M., Gordon, C. T., Griffies, S. M., Held, I. M., Hurlin, W. J., Klein, S. A., Knutson, T. R., Langenhorst, A. R., Lee, H.-C., Lin, Y., Magi, B. I., Malyshev, S. L., Milly, P. C. D., Naik, V., Nath, M. J., Pincus, R., Ploshay, J. J., Ramaswamy, V., Seman, C. J., Shevliakova, E., Sirutis, J. J., Stern, W. F., Stouffer, R. J., Wilson, R. J., Winton, M., Wittenberg, A. T., and Zeng, F.: The Dynamical Core, Physical Parameterizations, and Basic Simulation Characteristics of the Atmospheric Component AM3 of the GFDL Global Coupled Model CM3, J. Clim., 24, 3484–3519, 2011.

Freidenreich, S. M. and Ramaswamy, V.: A new multiple-band solar radiative parameterization for general circulation models, Journal of Geophysical Research: Atmospheres, 104, 31 389–31 409, doi:10.1029/1999jd900456, https://doi.org/10.1029/1999jd900456, 1999.

Ginoux, P., Chin, M., Tegen, I., Prospero, J. M., Holben, B., Dubovik, O., and Lin, S.-J.: Sources and distributions of dust aerosols simulated with the GOCART model, J. Geophys. Res. Atmos., 106, 20 255–20 273, 2001.

Ginoux, P., Prospero, J. M., Gill, T. E., Hsu, N. C., and Zhao, M.: Global-scale attribution of anthropogenic and natural dust sources and their emission rates based on MODIS Deep Blue aerosol products, Rev. Geophys., 50, RG3005, 2012.

Griffies, S. M., Winton, M., Donner, L. J., Horowitz, L. W., Downes, S. M., Farneti, R., Gnanadesikan, A., Hurlin, W. J., Lee, H.-C., Liang, Z., Palter, J. B., Samuels, B. L., Wittenberg, A. T., Wyman, B. L., Yin, J., and Zadeh, N.: The GFDL CM3 Coupled Climate Model: Characteristics of the Ocean and Sea Ice Simu-

lations, J. Clim., 24, 3520–3544, doi:10.1175/2011JCLI3964.1, http://journals.ametsoc.org/doi/abs/10.1175/2011JCLI3964.1, 2011.

Guenther, A., Karl, T., Harley, P., Wiedinmyer, C., Palmer, P. I., and Geron, C.: Estimates of global terrestrial isoprene emissions using MEGAN (Model of Emissions of Gases and Aerosols from Nature), Atmos. Chem. Phys., 6, 3181–3210, 2006.

Guo, H., Weber, R. J., and Nenes, A.: High levels of ammonia do not raise fine particle pH sufficiently to yield nitrogen oxide-dominated sulfate production, Scientific Reports, 7, doi:10.1038/s41598-017-11704-0, https://doi.org/10.1038/s41598-017-11704-0, 2017.

He, P., Alexander, B., Geng, L., Chi, X., Fan, S., Zhan, H., Kang, H., Zheng, G., Cheng, Y., Su, H., Liu, C., and Xie, Z.: Isotopic constraints on heterogeneous sulphate production in Beijing haze, Atmospheric Chemistry and Physics Discussions, pp. 1–25, doi:10.5194/acp-2017-977, https://doi.org/10.5194/acp-2017-977, 2017.

Heald, C. L., Ridley, D. A., Kroll, J. H., Barrett, S. R. H., Cady-Pereira, K. E., Alvarado, M. J., and Holmes, C. D.: Contrasting the direct radiative effect and direct radiative forcing of aerosols, Atmos. Chem. Phys., 14, 5513–5527, doi:10.5194/acp-14-5513-2014, http://www.atmos-chem-phys.net/14/5513/2014/, 2014.

Hoesly, R. M., Smith, S. J., Feng, L., Klimont, Z., Janssens-Maenhout, G., Pitkanen, T., Seibert, J. J., Vu, L., Andres, R. J., Bolt, R. M., Bond, T. C., Dawidowski, L., Kholod, N., Kurokawa, J.-I., Li, M., Liu, L., Lu, Z., Moura, M. C. P., O'Rourke, . P. R., and Zhang, Q.: Historical (1750–2014) anthropogenic emissions of reactive gases and aerosols from the Community Emissions Data System (CEDS), Geoscientific Model Development, 11, 369–408, doi:10.5194/gmd-11-369-2018, https://www.geosci-model-dev.net/11/369/2018/, 2018.

Hung, H.-M. and Hoffmann, M. R.: Oxidation of gas-phase SO_2 on the surfaces of acidic microdroplets: implications for sulfate and sulfate radical anion formation in the atmospheric liquid phase, Environ. Sci. Technol., 49, 13 768–13 776, doi:10.1021/acs.est.5b01658, http://dx.doi.org/10.1021/acs.est.5b01658, 2015.

Irie, H., Muto, T., Itahashi, S., Kurokawa, J.-i., and Uno, I.: Turnaround of Tropospheric Nitrogen Dioxide Pollution Trends in China, Japan, and South Korea, Sola, 12, 170–174, doi:10.2151/sola.2016-035, 2016.

John, J. G., Fiore, A. M., Naik, V., Horowitz, L. W., and Dunne, J. P.: Climate versus emission drivers of methane lifetime against loss by tropospheric OH from 1860–2100, Atmos. Chem. Phys., 12, 12 021–12 036, 2012.

Kahn, R. A.: Reducing the Uncertainties in Direct Aerosol Radiative Forcing, Surveys in Geophysics, 33, 701–721, doi:10.1007/s10712-011-9153-z, https://link.springer.com/article/10.1007/s10712-011-9153-z, 2012.

Kahn, R. A., Gaitley, B. J., Martonchik, J. V., Diner, D. J., Crean, K. A., and Holben, B.: Multiangle Imaging Spectroradiometer (MISR) global aerosol optical depth validation based on 2 years of coincident Aerosol Robotic Network (AERONET) observations, Journal of Geophysical Research: Atmospheres, 110, n/a–n/a, doi:10.1029/2004JD004706, http://dx.doi.org/10.1029/2004JD004706, d10S04, 2005.

Kahn, R. A., Gaitley, B. J., Garay, M. J., Diner, D. J., Eck, T. F., Smirnov, A., and Holben, B. N.: Multiangle Imaging SpectroRadiometer global aerosol product assessment by comparison with the Aerosol Robotic Network, Journal of Geophysical Research: Atmospheres, 115, n/a–n/a, doi:10.1029/2010JD014601, http://dx.doi.org/10.1029/2010JD014601, d23209, 2010.

Kalnay, E., Kanamitsu, M., Kistler, R., Collins, W., Deaven, D., Gandin, L., Iredell, M., Saha, S., White, G., Woollen, J., Zhu, Y., Leetmaa, A., Reynolds, R., Chelliah, M., Ebisuzaki, W., Higgins, W., Janowiak, J., Mo,

K. C., Ropelewski, C., Wang, J., Jenne, R., and Joseph, D.: The NCEP/NCAR 40-Year Reanalysis Project, Bull. Am. Meteorol. Soc., 77, 437–471, 1996.

Kendall, M. G.: A new measure of rank correlation, Biometrika, 30, 81–93, doi:10.1093/biomet/30.1-2.81, +http://dx.doi.org/10.1093/biomet/30.1-2.81, 1938.

Kim, D., Chin, M., Bian, H., Tan, Q., Brown, M. E., Zheng, T., You, R., Diehl, T., Ginoux, P., and Kucsera, T.: The effect of the dynamic surface bareness on dust source function, emission, and distribution, Journal of Geophysical Research: Atmospheres, 118, 871–886, doi:10.1029/2012JD017907, http://onlinelibrary.wiley.com/doi/10.1029/2012JD017907/abstract, 2013.

Krotkov, N. A., McLinden, C. A., Li, C., Lamsal, L. N., Celarier, E. A., Marchenko, S. V., Swartz, W. H., Bucsela, E. J., Joiner, J., Duncan, B. N., Boersma, K. F., Veefkind, J. P., Levelt, P. F., Fioletov, V. E., Dickerson, R. R., He, H., Lu, Z., and Streets, D. G.: Aura OMI observations of regional SO2 and NO2 pollution changes from 2005 to 2015, Atmos. Chem. Phys., 16, 4605–4629, doi:10.5194/acp-16-4605-2016, https://www.atmos-chem-phys.net/16/4605/2016/, 2016.

Kühn, T., Partanen, A.-I., Laakso, A., Lu, Z., Bergman, T., Mikkonen, S., Kokkola, H., Korhonen, H., Räisänen, P., Streets, D. G., Romakkaniemi, S., and Laaksonen, A.: Climate impacts of changing aerosol emissions since 1996, Geophysical Research Letters, 41, 4711–4718, doi:10.1002/2014gl060349, https://doi.org/10.1002/2014gl060349, 2014.

Levy, H., Horowitz, L. W., Schwarzkopf, M. D., Ming, Y., Golaz, J.-C., Naik, V., and Ramaswamy, V.: The roles of aerosol direct and indirect effects in past and future climate change, J. Geophys. Res. Atmos., 118, 4521–4532, 2013a.

Levy, R. C., Mattoo, S., Munchak, L. A., Remer, L. A., Sayer, A. M., Patadia, F., and Hsu, N. C.: The Collection 6 MODIS aerosol products over land and ocean, Atmospheric Measurement Techniques, 6, 2989–3034, doi:10.5194/amt-6-2989-2013, https://doi.org/10.5194/amt-6-2989-2013, 2013b.

Li, C., Zhang, Q., Krotkov, N. A., Streets, D. G., He, K., Tsay, S.-C., and Gleason, J. F.: Recent large reduction in sulfur dioxide emissions from Chinese power plants observed by the Ozone Monitoring Instrument, Geophysical Research Letters, 37, n/a–n/a, doi:10.1029/2010GL042594, http://dx.doi.org/10.1029/2010GL042594, l08807, 2010.

Liu, F., Zhang, Q., A, R. J. v. d., Zheng, B., Tong, D., Yan, L., Zheng, Y., and He, K.: Recent reduction in NO x emissions over China: synthesis of satellite observations and emission inventories, Environmental Research Letters, 11, 114 002, doi:10.1088/1748-9326/11/11/114002, http://stacks.iop.org/1748-9326/11/i=11/a=114002, 2016.

Liu, J., Fan, S., Horowitz, L. W., and Levy, H.: Evaluation of factors controlling long-range transport of black carbon to the Arctic, J. Geophys. Res. Atmos., 116, D04 307, 2011.

Loeb, N. G. and Manalo-Smith, N.: Top-of-Atmosphere Direct Radiative Effect of Aerosols over Global Oceans from Merged CERES and MODIS Observations, Journal of Climate, 18, 3506–3526, doi:10.1175/JCLI3504.1, http://journals.ametsoc.org/doi/abs/10.1175/JCLI3504.1, 2005.

Loeb, N. G., Wielicki, B. A., Doelling, D. R., Smith, G. L., Keyes, D. F., Kato, S., Manalo-Smith, N., and Wong, T.: Toward Optimal Closure of the Earth's Top-of-Atmosphere Radiation Budget, Journal of Climate, 22, 748–766, doi:10.1175/2008JCLI2637.1, http://journals.ametsoc.org/doi/abs/10.1175/2008JCLI2637.1, 2009.

Murphy, D. M.: Little net clear-sky radiative forcing from recent regional redistribution of aerosols, Nature Geoscience, 6, 258–262, doi:10.1038/ngeo1740, https://doi.org/10.1038/ngeo1740, 2013.

Myhre, G., Samset, B. H., Schulz, M., Balkanski, Y., Bauer, S., Berntsen, T. K., Bian, H., Bellouin, N., Chin, M., Diehl, T., Easter, R. C., Feichter, J., Ghan, S. J., Hauglustaine, D., Iversen, T., Kinne, S., Kirkevåg, A., Lamarque, J.-F., Lin, G., Liu, X., Lund, M. T., Luo, G., Ma, X., van Noije, T., Penner, J. E., Rasch, P. J., Ruiz, A., Seland, Ø., Skeie, R. B., Stier, P., Takemura, T., Tsigaridis, K., Wang, P., Wang, Z., Xu, L., Yu, H., Yu, F., Yoon, J.-H., Zhang, K., Zhang, H., and Zhou, C.: Radiative forcing of the direct aerosol effect from AeroCom Phase II simulations, Atmos. Chem. Phys., 13, 1853–1877, 2013.

Naik, V., Horowitz, L. W., Fiore, A. M., Ginoux, P., Mao, J., Aghedo, A. M., and Levy, H.: Impact of preindustrial to present-day changes in short-lived pollutant emissions on atmospheric composition and climate forcing, J. Geophys. Res. Atmos., 118, 8086–8110, 2013.

Oleson, K. W., Bonan, G. B., Schaaf, C., Gao, F., Jin, Y., and Strahler, A.: Assessment of global climate model land surface albedo using MODIS data, Geophysical Research Letters, 30, n/a–n/a, doi:10.1029/2002GL016749, http://dx.doi.org/10.1029/2002GL016749, 1443, 2003.

Pan, X., Chin, M., Gautam, R., Bian, H., Kim, D., Colarco, P. R., Diehl, T. L., Takemura, T., Pozzoli, L., Tsigaridis, K., Bauer, S., and Bellouin, N.: A multi-model evaluation of aerosols over South Asia: common problems and possible causes, Atmos. Chem. Phys., 15, 5903–5928, doi:10.5194/acp-15-5903-2015, https://www.atmos-chem-phys.net/15/5903/2015/, 2015.

Patadia, F., Gupta, P., and Christopher, S. A.: First observational estimates of global clear sky shortwave aerosol direct radiative effect over land, Geophysical Research Letters, 35, L04 810, doi:10.1029/2007GL032314, http://onlinelibrary.wiley.com/doi/10.1029/2007GL032314/abstract, 2008.

Paulot, F., Jacob, D. J., Pinder, R. W., Bash, J. O., Travis, K., and Henze, D. K.: Ammonia emissions in the United States, European Union, and China derived by high-resolution inversion of ammonium wet deposition data: Interpretation with a new agricultural emissions inventory (MASAGE_NH3), J. Geophys. Res. Atmos., 119, 4343–4364, 2014.

Paulot, F., Ginoux, P., Cooke, W. F., Donner, L. J., Fan, S., Lin, M.-Y., Mao, J., Naik, V., and Horowitz, L. W.: Sensitivity of nitrate aerosols to ammonia emissions and to nitrate chemistry: implications for present and future nitrate optical depth, Atmos. Chem. Phys., 16, 1459–1477, doi:10.5194/acp-16-1459-2016, http://www.atmos-chem-phys.net/16/1459/2016/, 2016.

Paulot, F., Fan, S., and Horowitz, L. W.: Contrasting seasonal responses of sulfate aerosols to declining SO_2 emissions in the Eastern U.S.: Implications for the efficacy of SO_2 emission controls, Geophys. Res. Lett., 44, 455–464, doi:10.1002/2016GL070695, http://dx.doi.org/10.1002/2016GL070695, 2016GL070695, 2017a.

Paulot, F., Paynter, D., Ginoux, P., Naik, V., Whitburn, S., Van Damme, M., Clarisse, L., Coheur, P.-F., and Horowitz, L. W.: Gas-aerosol partitioning of ammonia in biomass burning plumes: Implications for the interpretation of spaceborne observations of ammonia and the radiative forcing of ammonium nitrate, Geophysical Research Letters, 44, 2017GL074 215, doi:10.1002/2017GL074215, http://onlinelibrary.wiley.com/doi/10.1002/2017GL074215/abstract, 2017b.

Rayner, N. A., Parker, D. E., Horton, E. B., Folland, C. K., Alexander, L. V., Rowell, D. P., Kent, E. C., and Kaplan, A.: Global analyses of sea surface temperature, sea ice, and night marine air temperature since the

late nineteenth century, J. Geophys. Res. Atmos., 108, 4407, doi:10.1029/2002JD002670, http://dx.doi.org/10.1029/2002JD002670, 2003.

Rosenfeld, D., Andreae, M. O., Asmi, A., Chin, M., de Leeuw, G., Donovan, D. P., Kahn, R., Kinne, S., Kivekäs, N., Kulmala, M., Lau, W., Schmidt, K. S., Suni, T., Wagner, T., Wild, M., and Quaas, J.: Global observations of aerosol-cloud-precipitation-climate interactions, Reviews of Geophysics, 52, 2013RG000 441, doi:10.1002/2013RG000441, http://onlinelibrary.wiley.com/doi/10.1002/2013RG000441/abstract, 2014.

Rutan, D., Rose, F., Roman, M., Manalo-Smith, N., Schaaf, C., and Charlock, T.: Development and assessment of broadband surface albedo from Clouds and the Earth's Radiant Energy System Clouds and Radiation Swath data product, Journal of Geophysical Research: Atmospheres, 114, D08 125, doi:10.1029/2008JD010669, http://onlinelibrary.wiley.com/doi/10.1029/2008JD010669/abstract, 2009.

Rutan, D. A., Kato, S., Doelling, D. R., Rose, F. G., Nguyen, L. T., Caldwell, T. E., and Loeb, N. G.: CERES Synoptic Product: Methodology and Validation of Surface Radiant Flux, Journal of Atmospheric and Oceanic Technology, 32, 1121–1143, doi:10.1175/JTECH-D-14-00165.1, http://journals.ametsoc.org/doi/abs/10.1175/JTECH-D-14-00165.1, 2015.

Sayer, A. M., Munchak, L. A., Hsu, N. C., Levy, R. C., Bettenhausen, C., and Jeong, M.-J.: MODIS Collection 6 aerosol products: Comparison between Aqua's e-Deep Blue, Dark Target, and "merged" data sets, and usage recommendations, Journal of Geophysical Research: Atmospheres, 119, 13,965–13,989, doi:10.1002/2014JD022453, http://dx.doi.org/10.1002/2014JD022453, 2014JD022453, 2014.

Schaaf, C. B., Gao, F., Strahler, A. H., Lucht, W., Li, X., Tsang, T., Strugnell, N. C., Zhang, X., Jin, Y., Muller, J.-P., Lewis, P., Barnsley, M., Hobson, P., Disney, M., Roberts, G., Dunderdale, M., Doll, C., d'Entremont, R. P., Hu, B., Liang, S., Privette, J. L., and Roy, D.: First operational BRDF, albedo nadir reflectance products from MODIS, Remote Sensing of Environment, 83, 135–148, doi:10.1016/S0034-4257(02)00091-3, http://www.sciencedirect.com/science/article/pii/S0034425702000913, 2002.

Schwarzkopf, M. D. and Ramaswamy, V.: Radiative effects of CH4, N2O, halocarbons and the foreign-broadened H2O continuum: A GCM experiment, Journal of Geophysical Research: Atmospheres, 104, 9467–9488, doi:10.1029/1999jd900003, https://doi.org/10.1029/1999jd900003, 1999.

Sen, P. K.: Estimates of the Regression Coefficient Based on Kendall's Tau, Journal of the American Statistical Association, 63, 1379–1389, doi:10.1080/01621459.1968.10480934, http://www.tandfonline.com/doi/abs/10.1080/01621459.1968.10480934, 1968.

Stevens, B. and Schwartz, S. E.: Observing and Modeling Earth's Energy Flows, Surveys in Geophysics, 33, 779–816, doi:10.1007/s10712-012-9184-0, https://doi.org/10.1007/s10712-012-9184-0, 2012.

Stevens, B., Fiedler, S., Kinne, S., Peters, K., Rast, S., Müsse, J., Smith, S. J., and Mauritsen, T.: MACv2-SP: a parameterization of anthropogenic aerosol optical properties and an associated Twomey effect for use in CMIP6, Geosci. Model Dev., 10, 433–452, doi:10.5194/gmd-10-433-2017, https://www.geosci-model-dev.net/10/433/2017/, 2017.

Storelvmo, T., Leirvik, T., Lohmann, U., Phillips, P. C. B., and Wild, M.: Disentangling greenhouse warming and aerosol cooling to reveal Earth's climate sensitivity, Nature Geoscience, 9, 286–289, doi:10.1038/ngeo2670, http://www.nature.com/ngeo/journal/v9/n4/full/ngeo2670.html?foxtrotcallback=true, 2016.

675 Su, W., Loeb, N. G., Schuster, G. L., Chin, M., and Rose, F. G.: Global all-sky shortwave direct radiative forcing of anthropogenic aerosols from combined satellite observations and GOCART simulations, Journal of Geophysical Research: Atmospheres, 118, 655–669, doi:10.1029/2012jd018294, https://doi.org/10.1029/2012jd018294, 2013.

Tao, M., Chen, L., Wang, Z., Tao, J., Che, H., Wang, X., and Wang, Y.: Comparison and evaluation of the 680 MODIS Collection 6 aerosol data in China, Journal of Geophysical Research: Atmospheres, 120, 6992–7005, doi:10.1002/2015jd023360, https://doi.org/10.1002/2015jd023360, 2015.

Taylor, K. E., Williamson, D., and Zwiers, F.: The sea surface temperature and sea-ice concentration boundary conditions for AMIP II simulations, Program for Climate Model Diagnosis and Intercomparison, Lawrence Livermore National Laboratory, University of California, 2000.

685 Theil, H.: A rank-invariant method of linear and polynomial regression analysis. I, Nederl. Akad. Wetensch., Proc., 53, 386–392 = Indagationes Math. 12, 85–91 (1950), http://www.ams.org/mathscinet-getitem?mr=0036489, 1950.

Twomey, S.: Pollution and the planetary albedo, Atmospheric Environment, 8, 1251–1256, doi:10.1016/0004-6981(74)90004-3, http://www.sciencedirect.com/science/article/pii/0004698174900043, 1974.

690 van der A, R. J., Mijling, B., Ding, J., Koukouli, M. E., Liu, F., Li, Q., Mao, H., and Theys, N.: Cleaning up the air: effectiveness of air quality policy for SO_2 and NO_x emissions in China, Atmos. Chem. Phys., 17, 1775–1789, doi:10.5194/acp-17-1775-2017, https://www.atmos-chem-phys.net/17/1775/2017/, 2017.

van Marle, M. J. E., Kloster, S., Magi, B. I., Marlon, J. R., Daniau, A.-L., Field, R. D., Arneth, A., Forrest, M., Hantson, S., Kehrwald, N. M., Knorr, W., Lasslop, G., Li, F., Mangeon, S., Yue, C., Kaiser, J. W., and van der 695 Werf, G. R.: Historic global biomass burning emissions for CMIP6 (BB4CMIP) based on merging satellite observations with proxies and fire models (1750–2015), Geoscientific Model Development, 10, 3329–3357, doi:10.5194/gmd-10-3329-2017, https://doi.org/10.5194/gmd-10-3329-2017, 2017.

Vermote, E. F. and Kotchenova, S.: Atmospheric correction for the monitoring of land surfaces, Journal of Geophysical Research: Atmospheres, 113, D23S90, doi:10.1029/2007JD009662, http://onlinelibrary.wiley.700 com/doi/10.1029/2007JD009662/abstract, 2008.

Vermote, E. F. and Saleous, N.: Operational Atmospheric Correction of MODIS Visible to Middle Infrared Land Surface Data in the Case of an Infinite Lambertian Target, in: Earth Science Satellite Remote Sensing, pp. 123–153, Springer, Berlin, Heidelberg, https://link.springer.com/chapter/10.1007/978-3-540-37293-6_8, dOI: 10.1007/978-3-540-37293-6_8, 2006.

705 Vermote, E. F., El Saleous, N., Justice, C. O., Kaufman, Y. J., Privette, J. L., Remer, L., Roger, J. C., and Tanré, D.: Atmospheric correction of visible to middle-infrared EOS-MODIS data over land surfaces: Background, operational algorithm and validation, Journal of Geophysical Research: Atmospheres, 102, 17 131–17 141, doi:10.1029/97JD00201, http://onlinelibrary.wiley.com/doi/10.1029/97JD00201/abstract, 1997.

Vermote, E. F., El Saleous, N. Z., and Justice, C. O.: Atmospheric correction of MODIS data in the vis-710 ible to middle infrared: first results, Remote Sensing of Environment, 83, 97–111, doi:10.1016/S0034-4257(02)00089-5, http://www.sciencedirect.com/science/article/pii/S0034425702000895, 2002.

Wang, S., Xing, J., Jang, C., Zhu, Y., Fu, J. S., and Hao, J.: Impact Assessment of Ammonia Emissions on Inorganic Aerosols in East China Using Response Surface Modeling Technique, Environ. Sci. Technol., 45, 9293–9300, doi:10.1021/es2022347, http://dx.doi.org/10.1021/es2022347, 2011.

715 Wang, Y., Zhang, Q., Jiang, J., Zhou, W., Wang, B., He, K., Duan, F., Zhang, Q., Philip, S., and Xie, Y.: Enhanced sulfate formation during China's severe winter haze episode in January 2013 missing from current models, J. Geophys. Res. Atmos., 119, 2013JD021 426, doi:10.1002/2013JD021426, http://onlinelibrary.wiley.com/doi/10.1002/2013JD021426/abstract, 2014a.

Wang, Z., Schaaf, C. B., Strahler, A. H., Chopping, M. J., Román, M. O., Shuai, Y., Woodcock, C. E., 720 Hollinger, D. Y., and Fitzjarrald, D. R.: Evaluation of MODIS albedo product (MCD43A) over grassland, agriculture and forest surface types during dormant and snow-covered periods, Remote Sensing of Environment, 140, 60–77, doi:10.1016/j.rse.2013.08.025, http://www.sciencedirect.com/science/article/pii/S0034425713002836, 2014b.

Warner, J. X., Dickerson, R. R., Wei, Z., Strow, L. L., Wang, Y., and Liang, Q.: Increased atmospheric ammo- 725 nia over the world's major agricultural areas detected from space, Geophys. Res. Lett., p. 2016GL072305, doi:10.1002/2016GL072305, http://onlinelibrary.wiley.com/doi/10.1002/2016GL072305/abstract, 2017.

Wielicki, B. A., Barkstrom, B. R., Harrison, E. F., Lee, R. B., Louis Smith, G., and Cooper, J. E.: Clouds and the Earth's Radiant Energy System (CERES): An Earth Observing System Experiment, Bulletin of the American Meteorological Society, 77, 853–868, doi:10.1175/1520-0477(1996)077<0853:CATERE>2.0.CO;2, http: 730 //journals.ametsoc.org/doi/abs/10.1175/1520-0477(1996)077%3C0853%3ACATERE%3E2.0.CO%3B2, 1996.

Wielicki, B. A., Barkstrom, B. R., Baum, B. A., Charlock, T. P., Green, R. N., Kratz, D. P., Lee, R. B., Minnis, P., Smith, G. L., Wong, T., Young, D. F., Cess, R. D., Coakley, J. A., Crommelynck, D. A. H., Donner, L., Kandel, R., King, M. D., Miller, A. J., Ramanathan, V., Randall, D. A., Stowe, L. L., and Welch, R. M.: Clouds 735 and the Earth's Radiant Energy System (CERES): algorithm overview, IEEE Transactions on Geoscience and Remote Sensing, 36, 1127–1141, doi:10.1109/36.701020, 1998.

Wild, M.: Global dimming and brightening: A review, Journal of Geophysical Research: Atmospheres, 114, D00D16, doi:10.1029/2008JD011470, http://onlinelibrary.wiley.com/doi/10.1029/2008JD011470/abstract, 2009.

740 Wu, Y., de Graaf, M., and Menenti, M.: Improved MODIS Dark Target aerosol optical depth algorithm over land: angular effect correction, Atmospheric Measurement Techniques, 9, 5575–5589, doi:10.5194/amt-9-5575-2016, https://doi.org/10.5194/amt-9-5575-2016, 2016.

Xiao, Q., Zhang, H., Choi, M., Li, S., Kondragunta, S., Kim, J., Holben, B., Levy, R. C., and Liu, Y.: Evaluation of VIIRS,GOCI, and MODIS Collection 6 AOD retrievals against ground sunphotometer observations over 745 East Asia, Atmospheric Chemistry and Physics, 16, 1255–1269, doi:10.5194/acp-16-1255-2016, https://doi.org/10.5194/acp-16-1255-2016, 2016.

Xing, J., Mathur, R., Pleim, J., Hogrefe, C., Gan, C.-M., Wong, D. C., and Wei, C.: Can a coupled meteorology–chemistry model reproduce the historical trend in aerosol direct radiative effects over the Northern Hemisphere?, Atmos. Chem. Phys., 15, 9997–10 018, doi:10.5194/acp-15-9997-2015, https://www.atmos-chem-phys.net/15/9997/2015/, 2015. 750

Zhang, L., Chen, Y., Zhao, Y., Henze, D. K., Zhu, L., Song, Y., Paulot, F., Liu, X., Pan, Y., and Huang, B.: Agricultural ammonia emissions in China: reconciling bottom-up and top-down estimates, Atmos. Chem. Phys. Discuss., 2017, 1–36, doi:10.5194/acp-2017-749, https://www.atmos-chem-phys-discuss.net/acp-2017-749/, 2017.

Zhang, Q., Streets, D. G., Carmichael, G. R., He, K. B., Huo, H., Kannari, A., Klimont, Z., Park, I. S., Reddy, S., Fu, J. S., Chen, D., Duan, L., Lei, Y., Wang, L. T., and Yao, Z. L.: Asian emissions in 2006 for the NASA INTEX-B mission, Atmos. Chem. Phys., 9, 5131–5153, doi:10.5194/acp-9-5131-2009, https://www.atmos-chem-phys.net/9/5131/2009/, 2009.

Zhao, B., Jiang, J. H., Gu, Y., Diner, D., Worden, J., Liou, K.-N., Su, H., Xing, J., Michael Garay, and Huang, L.: Decadal-scale trends in regional aerosol particle properties and their linkage to emission changes, Environmental Research Letters, 12, 054 021, doi:10.1088/1748-9326/aa6cb2, http://stacks.iop.org/1748-9326/12/i=5/a=054021, 2017.

Zheng, B., Zhang, Q., Zhang, Y., He, K. B., Wang, K., Zheng, G. J., Duan, F. K., Ma, Y. L., and Kimoto, T.: Heterogeneous chemistry: a mechanism missing in current models to explain secondary inorganic aerosol formation during the January 2013 haze episode in North China, Atmos. Chem. Phys., 15, 2031–2049, doi:10.5194/acp-15-2031-2015, http://www.atmos-chem-phys.net/15/2031/2015/, 2015.

Zhu, Z., Piao, S., Myneni, R. B., Huang, M., Zeng, Z., Canadell, J. G., Ciais, P., Sitch, S., Friedlingstein, P., Arneth, A., Cao, C., Cheng, L., Kato, E., Koven, C., Li, Y., Lian, X., Liu, Y., Liu, R., Mao, J., Pan, Y., Peng, S., Peñuelas, J., Poulter, B., Pugh, T. A. M., Stocker, B. D., Viovy, N., Wang, X., Wang, Y., Xiao, Z., Yang, H., Zaehle, S., and Zeng, N.: Greening of the Earth and its drivers, Nature Climate Change, 6, 791–795, doi:10.1038/nclimate3004, https://doi.org/10.1038/nclimate3004, 2016.